NASA Technical Memorandum 104566, Vol. 15

SeaWiFS Technical Report Series

Stanford B. Hooker and Elaine R. Firestone, Editors

Volume 15, The Simulated SeaWiFS Data Set, Version 2

Watson W. Gregg, Frederick S. Patt, and Robert H. Woodward

January 1994

NASA Technical Memorandum 104566, Vol. 15

SeaWiFS Technical Report Series

Stanford B. Hooker, Editor
NASA Goddard Space Flight Center
Greenbelt, Maryland

Elaine R. Firestone, Technical Editor
General Sciences Corporation
Laurel, Maryland

Volume 15, The Simulated SeaWiFS Data Set, Version 2

Watson W. Gregg
NASA Goddard Space Flight Center
Greenbelt, Maryland

Frederick S. Patt and Robert H. Woodward
General Sciences Corporation
Laurel, Maryland

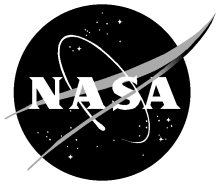

National Aeronautics and
Space Administration

Goddard Space Flight Center
Greenbelt, Maryland 20771

1994

Preface

In the prelaunch era of any space mission, simulated data sets are required in order to prove concepts of data formatting; mission health and safety; and mission operations including scheduling, transmission, and capture. Additionally, with a science mission like SeaWiFS, simulated data sets are necessary to test the ground data processing procedures and hopefully, test prelaunch science algorithms. Including the latter functions demands that the simulated data retain a high degree of fidelity to the data expected to be obtained. Producing such a data set for the simulation of scientific observations (including major geophysical variability based on global geophysical fields, sensor physics, and radiative transfer) is time consuming and requires the application of state-of-the-art scientific understanding of the entire remote sensing problem—from sensor physics to the final research algorithms.

Version 2 of the SeaWiFS data sets represents a major advance in the generation of a *complete* simulation. It has already proven extremely useful in testing various components of the SeaWiFS ground processing systems. Hopefully, it will prove valuable to other investigators and institutions who wish to process SeaWiFS data.

It will, however, be of limited use for the complete testing of level-2 and level-3 products with at-launch algorithms. By necessity, it makes use of the preliminary sensor radiometric responses and gain relationships. It is now clear that these will change significantly due to sensor modifications, which are required to minimize stray light effects. Final values of these parameters will be available only after several months from the submission date of this report. Whether there will be a Version 3 of the simulated data sets, including the at-launch sensor responses, has not yet been decided; it will depend upon resources, and how soon before launch the newer version could be ready. Being overtaken by events, in this case sensor modifications, is a risk borne by any simulation system.

Greenbelt, Maryland
September 1993

—W. E. Esaias
Project Scientist

Abstract

This document describes the second version of the simulated SeaWiFS data set. A realistic simulated data set is essential for mission readiness preparations and can potentially assist in all phases of ground support for a future mission. The second version improves on the first version primarily through additional realism and complexity. This version incorporates a representation of virtually every aspect of the flight mission. Thus, it provides a high fidelity data set for testing several aspects of the ground system, including data acquisition, data processing, data transfers, calibration and validation, quality control, and mission operations. The data set is constructed for a seven-day period, 25–31 March 1994. Specific features of the data set include Global Area Coverage (GAC), recorded Local Area Coverage (LAC), and real-time High Resolution Picture Transmission (HRPT) data for the seven-day period. A realistic orbit, which is propagated using a Brouwer-Lyddane model with drag, is used to simulate orbit positions. The simulated data corresponds to the command schedule based on the orbit for this seven-day period. It includes total (at-satellite) radiances not only for ocean, but for land, clouds, and ice. The simulation also utilizes a high-resolution land-sea mask. It includes the April 1993 SeaWiFS spectral responses and sensor saturation responses. The simulation is formatted according to July 1993 onboard data structures, which include corresponding telemetry (instrument and spacecraft) data. The methods are described and some examples of the output are given. The instrument response functions made available in April 1993 have been used to produce the Version 2 simulated data. These response functions will change as part of the sensor improvements initiated in July–August 1993.

1. INTRODUCTION

The availability of simulated data is essential for the preparation of a remote sensing mission. The usefulness of the simulated data for mission preparation activities depends upon the thoroughness with which the data are prepared, the adherence to format and content specifications, and the realism of the data. For example, data transfer speeds, storage capabilities, and computer memory requirements can usually be tested using dummy data sets of the expected volume. Unpacking algorithms, computer processing requirements, and intricacies of storing the data require that at least the correct data structures and formats are created in the simulated set. More advanced mission preparation activities, such as quality control, algorithm development, mission health and safety monitoring, and the initiation of an awareness of potential in-flight problems and discoveries, require a realistic data set containing observations similar to the expected flight data, with the correct volumes and structures. Such a simulated data set can potentially increase the success of the mission by exposing problems in sensor design, spacecraft operations, orbit anomalies, etc., well in advance of launch, allowing repair (if detected in time) or compensation by developing algorithms or revising the sensor and spacecraft operations scenario.

The development of a realistic simulated data set is simplified if a predecessor mission exists. If the predecessor mission is an exact copy of the future mission, then development of simulated data is simply a matter of using the previous data. This is rarely the case, however, since the predecessor mission often yields insights that lead to an improved sensor design and capability, or perhaps a different spacecraft or orbit configuration. In most cases, additional effort and data are required for development of the simulated data set.

The Sea-viewing Wide Field-of-view Sensor (SeaWiFS) mission, due for launch in 1994, is an example of a mission that has a highly successful predecessor sensor, the NIMBUS-7 Coastal Zone Color Scanner (CZCS), but contains many improvements in sensor design that render direct use of the predecessor data insufficient for mission preparation. The most important differences are the spectral band placement and the global, routine operations scenario for SeaWiFS, since CZCS was a limited duty sensor. Additional differences include the sensor scan parameters and the overall data content, especially the telemetry.

This method for constructing a simulated SeaWiFS data set takes advantage of the fact that the eight years of accumulated CZCS data led to many insights into the processes of radiative transfer in the ocean, and the relationship of these processes to remote sensing principles. By emphasizing this knowledge, a realistic simulated data set for a similar, but not identical, sensor may be developed without relying excessively on manipulation of previous, and only approximately valid, data sets.

The primary use of this simulated data set is to support SeaWiFS data system testing prior to launch. Thus, it attempts to include all information and characteristics to support processing and handling by all components of the SeaWiFS Project. The functions to be tested include, but are not limited to:

1) Transmission from the Wallops Flight Facility (WFF) to the Goddard Space Flight Center's

(GSFC) SeaWiFS Data Capture Facility (DCF);

2) Frame formatting of the data by the DCF and transfer to the SeaWiFS Data Processing System (SDPS);
3) Ingestion by the SDPS and generation of level-1a, level-2, and level-3 products, including navigation, atmospheric correction, and determination of geophysical parameters;
4) Quality control by the Calibration and Validation element, and navigation analysis by the Mission Operations element; and
5) The transfer of data products to the GSFC Distributed Active Archive Center (DAAC), where data are ingested, cataloged, and distributed.

The Version 2 simulated data relies upon April 1993 sensor responses. These response functions will change as part of sensor improvements initiated in July–August 1993; therefore, its value for testing level-2 and atmospheric correction is limited.

As is typical in the development of simulated data sets, the process proceeds in steps, each step building on the previous one in complexity and realism. The data set version presented in this paper is a direct descendant of Version 1 (Gregg et al. 1993). This version improves on Version 1 in the following ways:

a) Constructed for a seven-day period, 25–31 March 1994;
b) Includes all data types, i.e., Global Area Coverage (GAC), recorded Local Area Coverage (LAC) and real-time High Resolution Picture Transmission (HRPT) data for the seven-day period;
c) Data corresponds to a realistic command schedule for same seven-day period;
d) Includes total (at-satellite) radiances not only for ocean, but for land, clouds, and ice, and includes a high-resolution land-sea mask based on April 1993 (linear) response functions;
e) Includes preliminary SeaWiFS spectral responses and prelaunch sensor saturation responses provided by Hughes/Santa Barbara Research Corporation (SBRC), the instrument manufacturer;
f) Formatted according to revised and current (as of this writing) onboard data structures specified by Orbital Sciences Corporation (OSC), the spacecraft manufacturer;
g) Includes corresponding telemetry (instrument and spacecraft) data; and
h) Corresponds to a realistic orbit generated using a Brouwer-Lyddane model with drag.

Note that items d) and e) are outdated due to subsequent sensor improvements.

The methods for constructing the data set are described in the following, along with examples of data output.

2. BACKGROUND

The primary scientific goal of the SeaWiFS mission is to provide global monitoring of ocean color. However, because the spacecraft contains limited onboard storage capacity (119 Mbytes), onboard subsampling of the data is required to obtain global coverage. Thus, SeaWiFS will produce two different resolutions of data: LAC and GAC. LAC data is full sensor resolution (1 km), while GAC data is simply LAC data subsampled every fourth pixel along scan and along-track. GAC data also contains only data within a 45° swath width, in contrast to the 58.3° swath for LAC data. Since both of these data are stored on board the spacecraft data recorder, they are referred to as stored data. Characteristics of the SeaWiFS sensor and the SeaStar spacecraft are shown in Tables 1a and 1b.

Table 1a. SeaWiFS spectral bands and center wavelengths, shown with those of CZCS for comparison. Wavelengths (λ) are in nm.

SeaWiFS		*CZCS*	
Band No.	λ	Band No.	λ
1	412	1	443
2	443	2	520
3	490	3	550
4	510	4	670
5	555	5	750†
6	670	6	13.5μm‡
7	765		
8	865		

† Intended for surface vegetation analyses only (Williams et al. 1985).

‡ Data suspect after 1979 (Williams et al. 1985).

In addition to stored LAC and GAC data, SeaWiFS will broadcast real-time LAC data whenever the sensor is turned on. HRPT stations may capture these data whenever the spacecraft is visible. However, due to the agreement between the National Aeronautics and Space Administration (NASA) and OSC, these real-time LAC data will be encrypted: decryption methods will require either a commercial license from OSC, in which case the data may be decrypted in real time, or a research license from GSFC in which case a two-week delay in decryption will be enforced.

3. METHODS

An overview of the methods will contribute to clarity and understanding. First, orbit positions are generated for a seven-day period in March 1994, initiated by simulated SeaStar orbital elements. Then a command schedule, which specifies the data collection periods and sensor state,

Table 1b. Orbit and sensor characteristics for the SeaWiFS and the CZCS, shown for comparison.

Characteristic	*CZCS*	*SeaWiFS*
Altitude (km)	955	705
Period (minutes)	104.0	98.9
Inclination	99.28°	98.25°
Equator Crossing Time (local)	Noon	Noon
Node Type	Ascending	Descending
Scan Width	39.34°	58.3° (LAC); 45° (GAC)
Instantaneous Field of View (IFOV)	0.05°	0.09°
Ground IFOV at Nadir (km)	0.825	1.12
Pixels Along Scan	1,968	1,285 (LAC); 248 (GAC)
Scan Period (seconds)	0.134	0.167 (LAC); 0.667 (GAC)
Scan Plane Tilt	±20°	±20°
Scan Ground Coverage (km)	1,566	2,802 (LAC); 1,502 (GAC)
Maximum Spacecraft Zenith Angle	46.8°	70.8° (LAC); 51.7° (GAC)
Digitization (bits)	8	10

Table 2. Simulated NORAD two-line elements for the SeaStar orbit used for orbit propagation in the simulated data set. The important components are: day of year (seventh word, first row), drag term (10th word, first row), inclination (third word, second row), right ascension ascending node (fourth word, second row), eccentricity (fifth word, second row—assume preceding decimal point), argument of perigee (sixth word, second row), mean anomaly (seventh word, second row), mean motion (eighth word, second row), and orbit number (first four digits in ninth word, second row).

Line 1: `00000U␣93␣32␣␣A␣94␣80.00000000␣␣.00000380␣␣00000-0␣␣18855-3␣0␣␣3084`
Line 2: `00000␣␣98.2330␣178.3000␣0010000␣␣␣␣0.0000␣␣␣␣0.0000␣14.55400000␣29414`

is created from these orbit positions based upon a realistic data acquisition requirements scenario, including both routine observations and calibration activities. Then, for each data collection period, the orbit positions to navigate the pointing vectors to Earth locations, according to GAC and LAC sensor specifications and the tilt configuration, is used. The geolocated pixels are associated with a number of atmospheric, land, and oceanic data files to obtain their radiative characteristics. The pixels are determined to be either cloud and ice, land, or ocean, each of which has a different logical pathway for computing at-satellite radiance. Sensor configuration information is appended, such as tilt, gain, etc., along with orbit position and velocity. Telemetry fields are then inserted, using realistic values wherever possible, and dummy fields where not. Finally, the computed radiances are converted to digital counts and adjusted for the sensor saturation responses using the preliminary linear radiometric response function.

The data are stored in two formats: one corresponding to the onboard structure (10-bit science data), and the other corresponding to the ground system frame formatter output (10-bit words in 16 bits, but all other data as in the onboard structure). The frame formatter output is considered to be level-0, since it is the first product seen by the GSFC SDPS and research HRPT stations. The onboard structure is maintained only in the spacecraft flight recorder and at acquisition by the primary ground station, WFF.

3.1 Orbit Propagation

Orbit positions and velocities are computed using a modified Brouwer-Lyddane model, with atmospheric drag included. The model is the Simplified General Perturbations Model (SGP4), distributed by the US Space Command. Simulated North American Air Defense Command two-line elements were created for the SeaStar orbit (Table 2) in the so-called NORAD Two-Line Element format, assuming the originally planned launch date of August 1993. The orbit positions and velocities are required for the geolocation step of the simulation, and are also included in the telemetry to simulate Global Positioning System (GPS) data, which are included in the SeaWiFS data.

3.2 Navigation

For Version 2, perfect spacecraft attitude control is assumed, and thus roll, pitch, and yaw are set to zero. The tilt configuration involves tilting aft of the velocity vector (toward the North Pole), and changing to fore (toward the South Pole) near the solar declination latitude to minimize sun glint contamination. Geolocation is achieved using an exact algorithm employing vector algebra, developed for SeaWiFS navigation (Patt and Gregg 1993).

3.3 Command Schedules

The sensor command schedules used for the simulation correspond to the orbit position data generated for

the period 25–31 March 1994, and incorporate a routine operations scenario, including GAC observations and calibration activities. The events included in the command schedule are:

1) GAC and LAC record times, including calibration times;
2) real-time HRPT data broadcast times;
3) recorded data downlink times;
4) tilt change times; and
5) sensor configuration for each event.

The process of scheduling begins with knowledge of down-link orbits at WFF. The mission requires two downlinks per day at WFF for full Earth coverage—one near local noon and one near local midnight. The local midnight pass always occurs first in each Greenwich Mean Time (GMT) day as a consequence of the orbit. During flight operations, these will be selected by WFF personnel, who must perform conflict resolution to maximize the acquisition requirements for many spacecraft. For simulation, the orbits are determined by selecting downlink orbits that provide a variety of expected conditions, i.e., as few as six orbits of data collection between downlinks to a maximum of more than nine orbits of data collection (Table 3). The orbit numbers in the table are based on the August 1993 launch date and the late March simulation dates. The selection of downlink orbits to produce variety in data collection schedules simulates a realistic scenario for SeaStar, which is only one of many spacecraft using WFF as the primary data acquisition station.

Given downlink orbits, the GAC recorder is then scheduled. A 40 minutes-per-orbit maximum duty cycle is adhered to, as determined by SeaStar power constraints. This duty cycle corresponds to a maximum solar zenith angle of 72.7°, which is the actual limit used in the scheduling software for GAC data collection. A series of commands is required to configure the instrument and flight recorder for start up and shutdown, and is included in the schedule. A sample portion of a command schedule is shown in Table 4.

Next, individual channel gains and Time Delay and Integration (TDI) settings are selected to maximize the scientific usefulness of the data being collected. For Earth-viewing observations, gains are set to unity and TDIs are set to zero, meaning that all four detectors per band are being used to increase the signal-to-noise ratio (SNR). During lunar, solar, intergain, and detector calibration events, gain and TDI settings follow specific instructions (Woodward et al. 1993), which are discussed below. The available gain settings for Version 2 are shown in Table 5.

The tilt strategy employed in the command schedules for the simulation data set involves a single tilt change on the descending node. The location of the tilt change is set to minimize sun glint contamination. In flight, the recommendation of Gregg and Patt (1993), which is called the "staggered tilt" strategy, will be followed. This strategy shifts the tilt change location a few degrees north of the maximum sun glint point (near the solar declination latitude) for two days, then shifts the position a few degrees south for the next two days. Gregg and Patt (1993) showed that this strategy improves the ocean coverage over a four-day period while simultaneously reducing sun glint contamination.

Table 3. Downlink orbit numbers at Wallops used in the command schedule construction.

Orbit Number	*Day of Year*
3002	84
3010	84
3017	85
3024	85
3031	86
3038	86
3046	87
3053	87
3060	88
3067	88
3074	89
3083	89
3090	90
3096	90

The SeaWiFS instrument tilt can be commanded to zero (nadir), 20° forward and 20° aft. For the SeaWiFS convention, an aft 20° tilt (opposite the velocity vector) is defined as +20°, and a forward tilt is defined as −20°. Note that the tilt changes are not instantaneous, but require approximately 13 seconds to complete, with tilt change rates that vary continuously during this period (Fig. 1). The sensor tilt position during a tilt change is computed using a mathematical fit to the SBRC data:

$$T = a \tanh(bt) \tag{1}$$

where T is the tilt position in degrees, t is the time in seconds and

$$a = \frac{-20}{\tanh(2)}, \tag{2}$$

$$b = \frac{1}{3}. \tag{3}$$

The LAC data capacity is determined by the total capacity of the flight recorder and the GAC storage requirements. Calibration and other LAC recording periods must be constrained by the available LAC space. Calibration requirements for the simulation run are derived from a simulated LAC target file. During the mission, this file will be supplied to the Mission Operations team by the Calibration and Validation team. There are five types of calibration activities in the SeaWiFS mission. These are, in order of priority: lunar calibration, solar calibration,

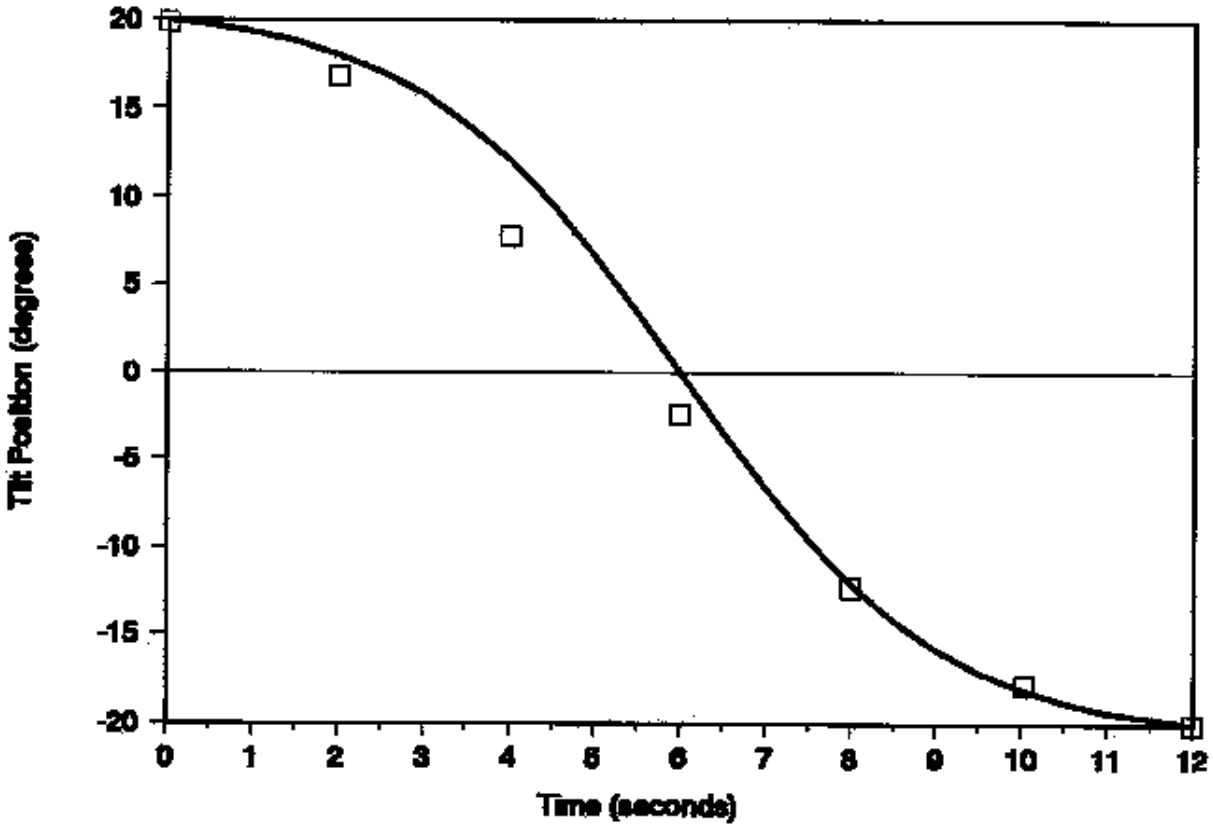

Fig. 1. Comparison of SBRC measured sensor tilt change response (squares) and mathematical fit used in the simulated data (line).

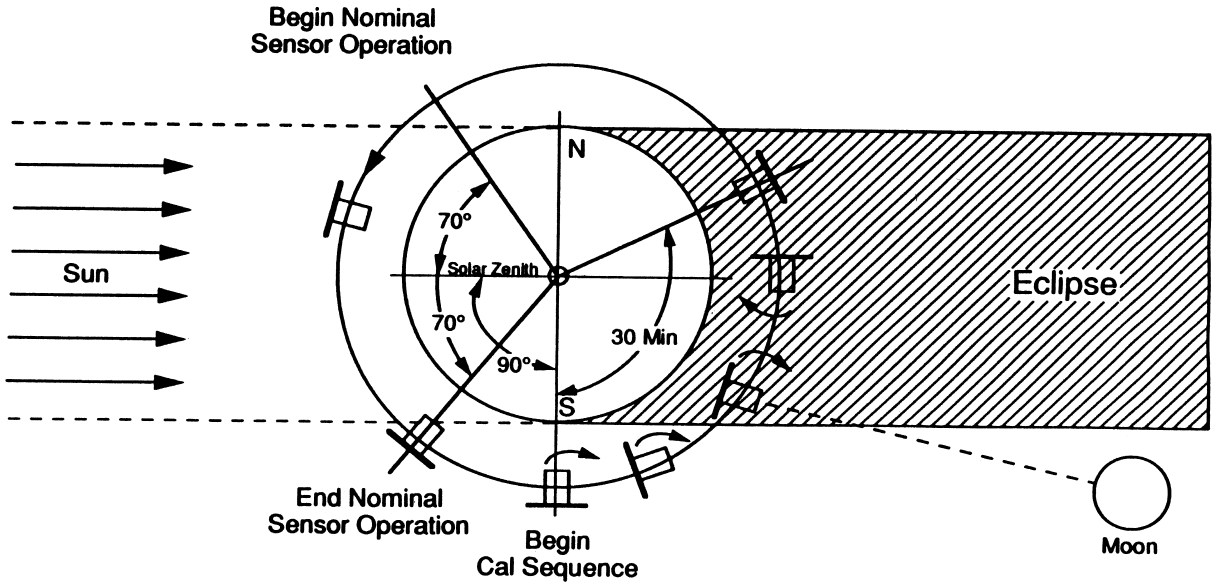

Fig. 2. Lunar calibration maneuver (courtesy of Orbital Sciences Corp.).

Table 4. Sample portion of the schedule for day of year 84.

Command	*Setting*	*Year*	*Day*	*Time*	*Orbit*	*Latitude*	*Sun*
L-band Transmitter Turn On	1	1994	84	604	2999	72.32°	72.7°
Reset Tilt Aft Position	20	1994	84	634	2999	72.32°	72.7°
Set Earth Mode On	1	1994	84	639	2999	72.32°	72.7°
Electronics Turn On Power	1	1994	84	654	2999	72.32°	72.7°
Change Gain Band 1, 2,. . .,8	1	1994	84	659	2999	72.32°	72.7°
Change TDI Band 1, 2,. . .,8	0	1994	84	660	2999	72.32°	72.7°
LAC Transmitting Turn On	1	1994	84	663	2999	72.32°	72.7°
GAC Recorder Turn On	1	1994	84	663	2999	72.32°	72.7°
LAC Recorder Turn On	1	1994	84	864	2999	61.27°	62.1°
LAC Recorder Turn Off	0	1994	84	894	2999	59.22°	62.1°
LAC Recorder Turn On	1	1994	84	1680	2999	12.57°	13.5°
Change Tilt To Forward	−20	1994	84	1855	2999	1.55°	0.4°
LAC Recorder Turn Off	0	1994	84	1860	2999	0.30°	1.7°
GAC Recorder Turn Off	0	1994	84	3063	2999	−69.47°	72.7°
LAC Transmitting Turn Off	0	1994	84	3063	2999	−69.47°	72.7°
L-band Transmitter Turn Off	0	1994	84	3065	2999	−69.47°	72.7°
Electronics Turn Off Power	0	1994	84	3066	2999	−69.47°	72.7°

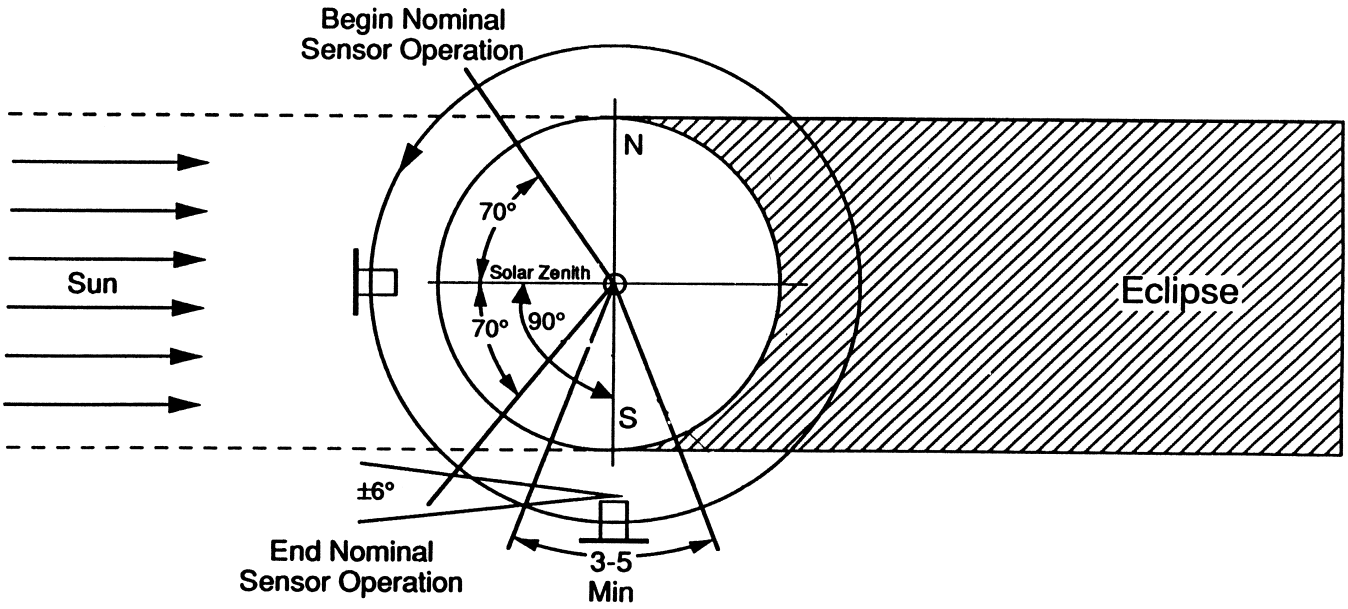

Fig. 3. Solar calibration maneuver (courtesy Orbital Sciences Corporation).

intergain check, detector check, and *in situ* LAC target observations. For this simulation, the file contains instructions to include one solar calibration per day, which includes an intergain check, and one detector check per day. A full moon occurs during the simulation period, on 27 March 1994, so a lunar calibration event is also scheduled.

The file also includes several ship, buoy, and region targets with an accompanying prioritization (Table 6). These requirements are implemented in data collection via the command schedule.

Lunar calibration is achieved by pitching the spacecraft 360° on the dark side of the orbit to view a moon near full phase (Fig. 2). The SeaWiFS Project has chosen a 7° lunar phase angle for lunar calibration (Woodward et al. 1993) to ensure calibration consistency and availability (smaller phase angles do not always occur in a given month). The specific time of the moon view is predicted based on the spacecraft position at the start of the pitch maneuver and the selected pitch rate. The pitch rate has been selected to collect about 20 LAC lines including moon data. The LAC recorder is turned on for two minutes total, centered on the predicted viewing time, to allow for uncertainties in the spacecraft pitch rate. Specific gain settings are utilized to prevent saturation and to ensure maximum dynamic range (Table 5).

Table 5. Gain settings for SeaWiFS.

Band	*Gain 1*	*Gain 2*	*Gain 3*	*Gain 4*
412	1	2^3	1.7^3	1.3
443	1	2	1.7^3	1.3
490	1	2	1.7	1.25
510	1^1	2	1.7	1.25^2
555	1^2	2	1.6^1	0.77
670	1	2	0.7^1	0.46^2
765	1	2	0.61^1	0.32^2
865	1	2	0.55^1	0.26^2

1. Used for lunar calibration.
2. Used for solar calibration.
3. Used for both lunar and solar calibration.

Solar calibration involves tilting the sensor 20° aft of the velocity vector when the spacecraft is at the southern terminator to view reflection off a solar diffuser plate mounted on the sensor (Fig. 3). The instrument is commanded into a unique *solar mode* configuration, which causes the sensor to sample a different part of the scan circle to allow a view of the diffuser plate, although, the LAC scan line still consists of 1,285 science pixels. Again, specific gain settings are used to maximize the scientific usefulness of the solar irradiance scattered off the diffuser plate (Table 5). The solar mode also includes an internal calibration signal. During each scan, after viewing the diffuser plate, the sensor electronics receives a constant-magnitude electronic pulse, called the calibration pulse, which enables a highly consistent intergain check to be performed. This check is performed immediately after the full solar calibration, using a specific sequence of channel gains (Table 7).

Detector checks also use the solar diffuser plate, and are performed on the orbit following the solar calibration activity. Again, a specific TDI and gain sequence is used (Table 8).

Finally, the remaining LAC recorder space is used to schedule *in situ* calibration targets. A distinction is made between two types of *in situ* targets for the SeaWiFS mission: ship and buoy targets, and region targets. Ship and buoy targets are discrete locations which have the higher priority of the two *in situ* types. For ship and buoy targets, the LAC recorder is turned on 15 seconds before viewing the target, and left on for 15 seconds after the target. This 30 second viewing duration provides 100 km of observations about the target. For regions, the recorder is turned on only if the sub-satellite point is within the region. This ensures that at least half the scan is in the region of interest. In this simulated data set, not all the available LAC space is used, due to the prototype status of the scheduling algorithms and code, which are under development and testing. For the mission, all available LAC space will be used.

3.4 Determining At-Satellite Radiances

At-satellite radiances are derived from five backscattering sources: clouds, land, ice, non-cloud atmosphere, and the ocean. In each case, the method for computing radiances involves the assumed known reflectance properties of the contributing source; solar geometry, which is dependent on the year, time of day, and position; and scan geometry, which is dependent on the simulated orbit position and known scanning characteristics of the sensor. Intensive radiative transfer calculations translate this knowledge into quantitative radiances taking into account the specific optical responses of the SeaWiFS sensor available as of April 1993. The calculations have not yet been made for a bilinear instrument response.

The calculation of at-satellite radiances thus begins with a determination of the state of the atmosphere, land, and oceans at the time of observation. This is obtained through the use of several global data sets. The same seven-day period in March 1990 for each data set was chosen to ensure coherence among the state variables. The data sets include information on cloud cover, ice cover, land vegetation, ocean chlorophyll concentration, wind speeds, surface pressure, and ozone concentration (Table 9). Each of these variables affects SeaWiFS observations:

1) Cloud cover determines the ability of the sensor to view the Earth and also determines the amount of saturation;
2) Ice cover and land vegetation affect the optical properties of land;
3) Ocean chlorophyll concentration contributes to the determination of the spectral properties of water-leaving radiance;

Table 6. LAC target file used for the simulated SeaWiFS data set. *In situ* targets have longitude and latitude associated with them, plus a priority indicator. Calibration activities are associated with a number indicating the number of such activities per month.

```
Calibration Targets
1994 82
In situ
 10
 Clark's Buoy              -156.3400       18.6700          4
 Bermuda Buoy               -71.9000       32.1200          6
 JGOFS                       63.2500       19.4000          3
 NOAA S. Atlantic Bight     -77.5200       32.0300          4
 NOAA Gulf of Cal.         -107.2600       22.1100          5
 S. Africa                   10.2300      -32.8700          6
 Galapagos                  -92.6200       -3.2500          8
 Gulf of Mexico             -86.8600       24.7900          3
 Oregon St.                -131.1400       45.7700          1
 Navy Bering Sea           -175.5800       63.4200         10
Regions
 5
 Sargasso Sea               -70.0000      -45.0000       20.0000      30.0000      2
 Gulf of Mexico            -110.0000      -80.0000       17.0000      31.0000      1
 SE Pacific                -150.0000      -90.0000      -60.0000     -30.0000      3
 Galapagos                 -105.0000      -75.0000      -15.0000       0.0000      5
 Micronesia                 135.0000      180.0000        0.0000      15.0000      4
Solar Calibration
 30
Lunar Calibration
 1
Intergain Calibration
 30
TDI Check
 30
```

4) Wind speeds determine the aerosol type over the oceans and the sun glint radiance magnitudes;
5) Surface pressure affects the Rayleigh scattering of the atmosphere and the oxygen concentration which absorbs irradiance and radiance in some SeaWiFS bands; and
6) Ozone concentrations affect the spectral transmittance of irradiance and radiance through the atmosphere.

The effect of water vapor on SeaWiFS bands is small, and so is set to a global mean of 1.5 cm. As stated above, the simulation procedure includes orbit propagation and navigation to determine the position of each pixel. The pixel's position is associated with the known position of each variable in the data sets, enabling knowledge of the current state. Examples of cloud and ice cover used are shown in Figs. 4 and 5.

Given knowledge of the state of the atmosphere and surface, and the pixel under examination in a full orbit propagation, the radiative properties are determined next. For cloud and ice cover, concentrations greater than 50% means that obscuration of the surface is assumed and the at-satellite radiance is computed as:

$$L_t(\lambda) \;=\; \frac{\rho_{c,i} E_d(\lambda, \theta_0)}{\pi}, \qquad (4)$$

where L_t is the total radiance received by the satellite (at-satellite radiance), ρ is the reflectance of clouds (subscript c) and ice (subscript i), and E_d is the incident irradiance on the Earth's surface as a function of the Earth-sun distance and atmospheric transmittance. The atmospheric transmittance properties are determined by the solar zenith angle, θ_0, which is known at each pixel from orbit position, pointing knowledge, and geolocation. Division by π enforces a Lambertian scattering assumption. For both clouds and ice, ρ is set to 1, i.e., clouds and ice are completely reflecting.

The incident irradiance is computed using the method of Gregg and Carder (1990), where extraterrestrial irradiance and other atmospheric optical properties are weighted to conform to the latest SeaWiFS spectral responses (Table 10). If a pixel is found to be greater than 50% ice or

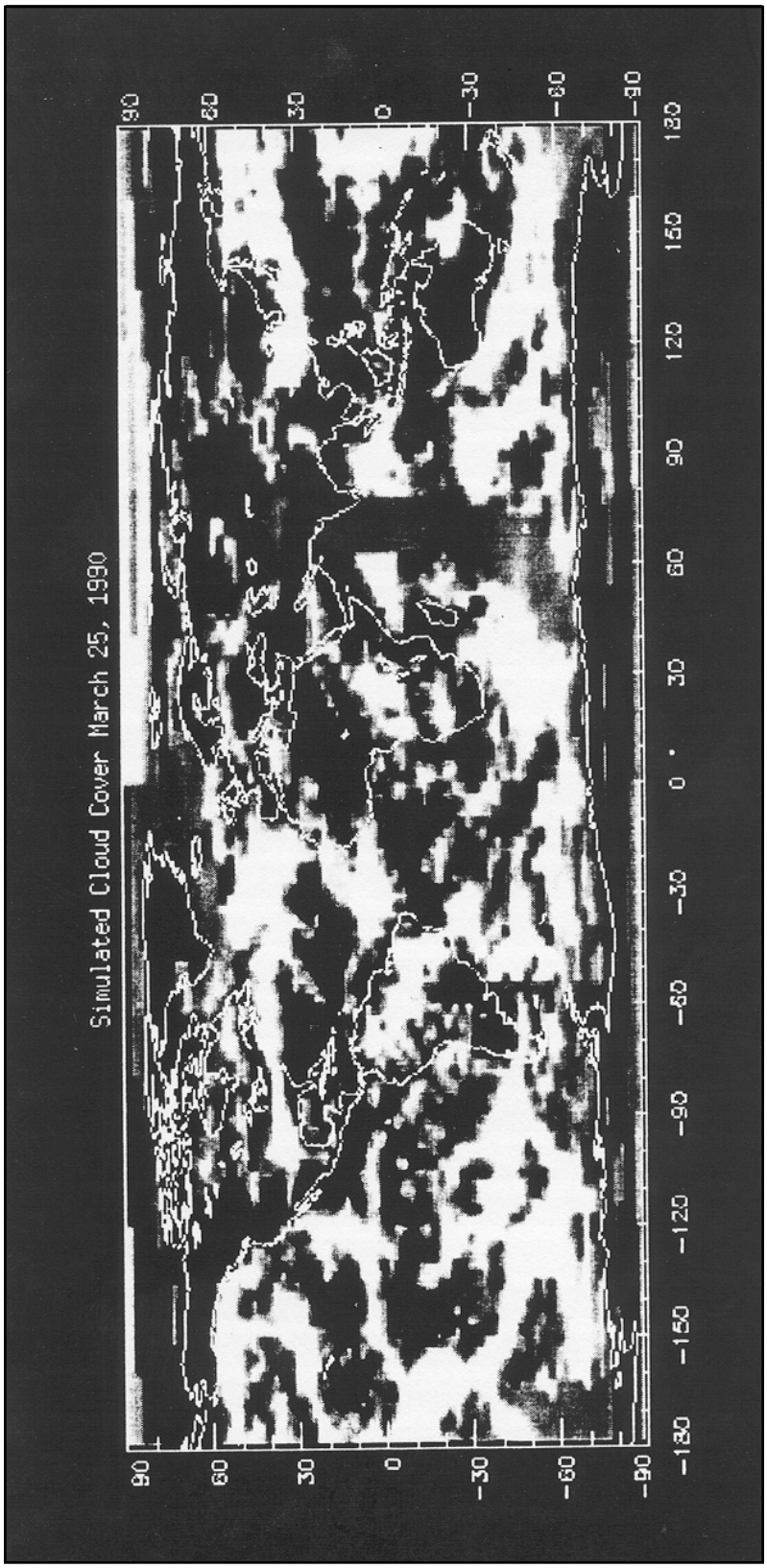

Fig. 4. Global cloud cover for 25 March 1990, derived from ISCCP data. Region is shown as clear if cloud cover is less than 50%.

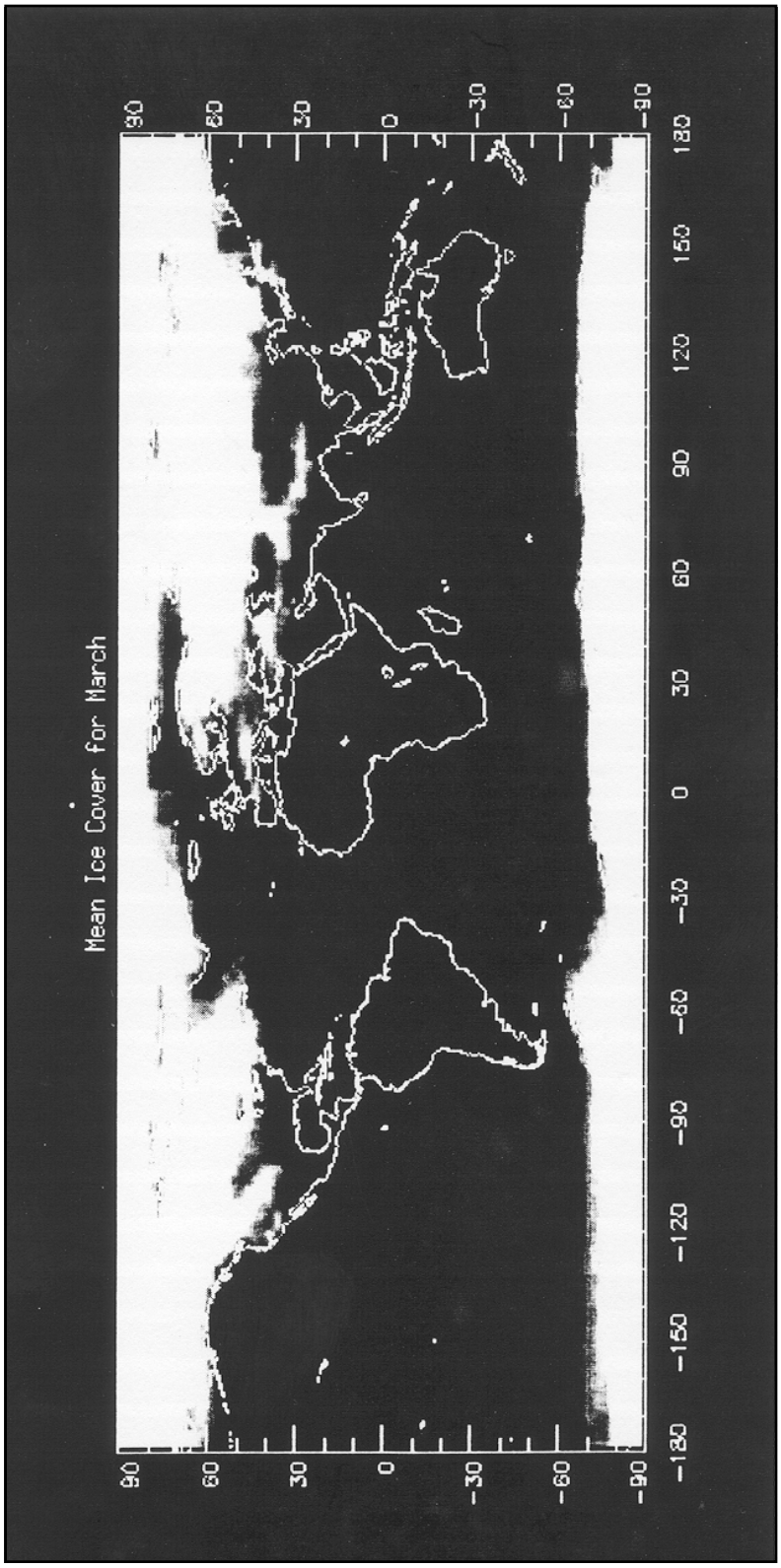

Fig. 5. Mean ice cover for March, derived from ISCCP data. Region is shown as clear if ice cover is less than 50%.

cloud, (4) is utilized and no further calculations are performed, under the assumption that the high reflectance properties of ice and clouds overwhelm other atmospheric, non-ice land, and oceanic contributions. If a pixel is found to be non-cloudy and non-ice, then it must be determined whether the pixel is land or ocean. This determination is made using a high resolution land-sea mask, which is derived from the World Vector Shoreline (WVS) Database, available from the National Geophysical Data Center (NGDC). The resolution of the land or sea mask is 128 pixels per degree of latitude or longitude, corresponding to 0.9 km at the equator, or slightly better than the LAC resolution. If the pixel under observation is found to be land, then the land radiance determination method is employed. Otherwise, the ocean radiance determination method is used.

Table 7. Command sequence for intergain check.

Gain 1, Gain 2, Gain 1, Gain 3, Gain 1, Gain 4, Gain 1
This gain sequence is repeated for each of 5 TDI configurations: 1. Use of all four detectors 2. Use of Detector 1 only 3. Use of Detector 2 only 4. Use of Detector 3 only 5. Use of Detector 4 only
The overall pattern is repeated once, along with a final repeat using all four detectors, requiring a total of 77 seconds to complete.

Table 8. Command sequence for a TDI check. This sequence is performed using solar calibration gains on all bands, since the check occurs in solar mode using the solar diffuser plate. Unique TDI configuration codes are defined by OSC, and these are used in the simulated data set.

TDI Configuration Code	*Meaning*
0	All 4 detectors
164	Detector 1 only
0	
26	Detector 2 only
0	
74	Detector 3 only
0	
161	Detector 4 only
0	
The pattern is repeated 9 times, requiring 81 seconds	

The land radiance determination method begins with the Advanced Very High Resolution Radiometer (AVHRR) reflectance data set. First, it is assumed that the reflectance of AVHRR band 1 (centered at 640 nm) equals the reflectance at SeaWiFS band 6 (670 nm). The Normalized Difference Vegetation Index (NDVI) is then computed. If the NDVI is greater than 0.2, the pixel is vegetated, and it is assumed that the reflectance at AVHRR band 2 (centered at 850 nm) equals the reflectances at SeaWiFS bands 7 and 8 (765 and 865 nm, respectively).

Table 9. External data sets used in the creation of simulated SeaWiFS data and their sources.

External Data Set	*Source*
Chlorophyll	Global CZCS composite (CZCS Global Reprocessing)
Land Vegetation	10-day AVHRR composite from April 1988 (AVHRR Pathfinder)
Wind Speed and Surface Pressure	FNOC data from 25–31 March 1990 (NCDS)
Clouds	ISCCP from 25–31 March 1990 (NCDS)
Ice	ISCCP climatological mean (NCDS)
Ozone	TOMS from 25–31 March 1990

Table 10. Spectrally weighted (FWHM) mean extraterrestrial irradiance $F_0(\lambda)$ (mW cm^{-2} μm^{-1}), Rayleigh optical thickness (τ_r), ozone absorption coefficient ($a_{\rm oz}$), water vapor absorption coefficient ($a_{\rm wv}$), and oxygen absorption coefficient ($a_{\rm o}$). All units are in cm^{-1}, except τ_r, which is dimensionless.

λ	F_0	τ_r	$a_{\rm oz}$	$a_{\rm wv}$	$a_{\rm o}$
410	171.07	0.3139	0.0000	0.0000	0.0000
443	189.91	0.2341	0.0030	0.0000	0.0000
490	194.33	0.1561	0.0213	0.0000	0.0000
510	188.24	0.1324	0.0382	0.0000	0.0000
555	185.93	0.0942	0.0897	0.0008	0.0000
670	152.14	0.0439	0.0470	0.0043	0.0053
765	123.55	0.0257	0.0083	0.0007	3.3780
865	100.00	0.0155	0.0000	0.0057	0.0000

Reflectances are then computed at SeaWiFS bands 1–5 as an inverse function of chlorophyll absorption coefficients weighted by the SeaWiFS spectral response, where the magnitude conforms to the reflectance at band 6. Values for chlorophyll absorption are taken from Gregg et al. (1993). If the NDVI is less than 0.2, the pixel is non-vegetated, and the slope is computed from AVHRR band 2 minus AVHRR band 1. A linear reflectance response, through SeaWiFS bands 1–5, is assumed following this slope. This method provides reasonable agreement with observations for two arbitrarily selected vegetated and non-vegetated points (Fig. 6). The reflectances are converted to at-satellite radiances as in (4), with the reflectance determined above substituted for $\rho_{c,i}$. Note that this method does not explicitly account for the atmosphere, although some is implicit in the AVHRR reflectances which do not correct for the atmosphere, nor for scan angle.

The ocean radiance method is described in great detail in Gregg et al. (1993) and will not be elaborated upon in

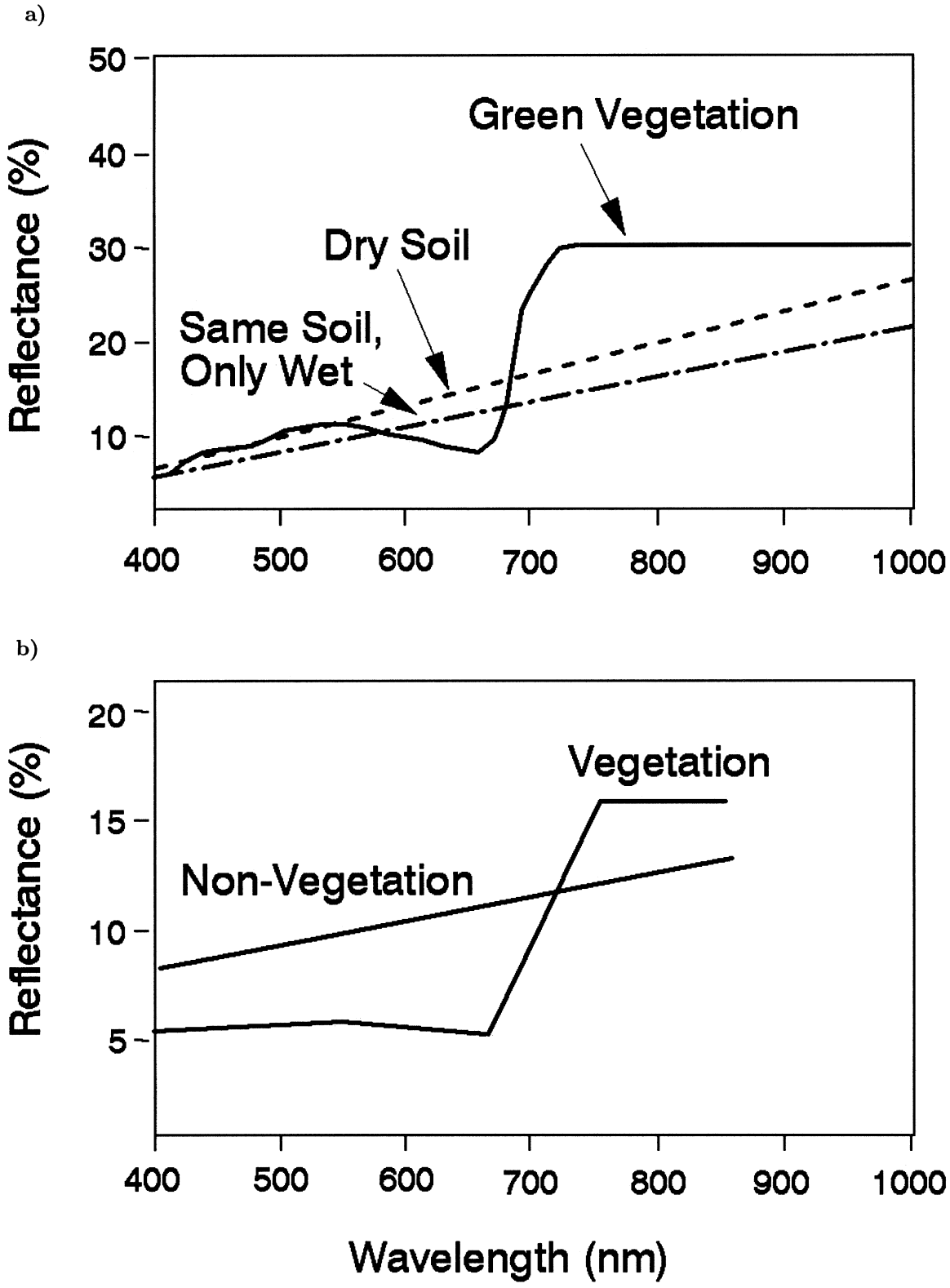

Fig. 6. a) Land reflectance data from Tucker and Miller (1978). **b)** Simulated land reflectances from AVHRR data for a vegetated location near the Nicaraguan and Costa Rican border, and for a non-vegetated location in the Mexican plateau (redrawn with permission from J. Tucker).

this document. There are, however, three significant differences in the method used here. First, wind speeds are taken from Fleet Numerical Oceanographic Center (FNOC) data for 25–31 March 1990, rather than using the climatological mean as in Gregg et al. (1993). Second, pressure effects are explicitly accounted for in the computation of multiple Rayleigh scattering through

$$I'(\lambda) \;=\; I_o(\lambda)\frac{1-e^{-\tau_r'(\lambda)M(\theta)}}{1-e^{-\tau_{ro}(\lambda)M(\theta)}}, \qquad (5)$$

where $I_0(\lambda)$ is the Rayleigh scattering intensity at standard pressure (Gordon et al. 1988), τ_{ro} is the Rayleigh optical thickness weighted by the SeaWiFS spectral response, and M is the slant path length through the atmosphere (see Gregg et al. 1993). The term τ_r' is the pressure-corrected optical thickness

$$\tau_r' \;=\; \tau_{ro}\frac{P}{P_0}, \qquad (6)$$

where P and P_0 are the local surface pressure and the standard pressure, respectively. Finally, the factor 4π is eliminated in the denominator of (28) in Gregg et al. (1993), since it is already accounted for in (30) of that reference. This error produced incorrectly low aerosol radiances in Version 1.

3.5 Conversion to Digital Counts

SeaWiFS simulated total radiance data were converted into digital counts by

$$DC(\lambda,G) \;=\; 20+\frac{L_t(\lambda)-L_{\rm NER}(\lambda,G)}{s(\lambda,G)}, \qquad (7)$$

where DC is the digital count value, $L_{\rm NER}(\lambda,G)$ is the Noise Equivalent Radiance (NER) as a function of wavelength and gain factor G, and s is the slope for the range 0–1,023. This is applicable for 10-bit digitization, given by

$$s(\lambda,G) \;=\; \frac{L_{\rm sat}(\lambda,G)-L_{\rm NER}(\lambda,G)}{1003}, \qquad (8)$$

where $L_{\rm sat}(\lambda,G)$ is the saturation radiance for the sensor as a function of wavelength and gain setting. $L_{\rm NER}(\lambda,G)$ and $L_{\rm sat}(\lambda,G)$ for Gain 1 are shown in Table 11. The addition of 20 counts in (7) represents the dark restore value used in the simulation. In flight, a dark restore value will be contained in the data stream and will be applicable for each scan line. This dark restore value also accounts for the division by 1,003 in (7), rather than division by 1,023.

Application of (7) and (8) does not truncate the data to 10-bit quantization. In the first run of the simulation data set, this is desirable, since it provides knowledge of the extent of saturation (number of counts above 1,023), which is required for determination of the sensor saturation responses. After the saturation responses are accounted for, the final simulation data set values are truncated to a maximum count value of 1,023.

Table 11. $L_{\rm NER}$ and saturation radiances ($L_{\rm sat}$) for SeaWiFS (units are mW cm^{-2} μm^{-1} sr^{-1}). $L_{\rm sat}$ will change in the launch configuration due to instrument modifications.

Band	λ [nm]	$L_{\rm NER}$	$L_{\rm sat}$
1	412	0.0094	13.63
2	443	0.0085	13.25
3	490	0.0055	10.50
4	510	0.0050	9.08
5	555	0.0041	7.44
6	670	0.0037	4.20
7	765	0.0022	3.00
8	865	0.0015	2.13

3.6 Sensor Saturation Response

The preliminary April 1993 test data from the SeaWiFS sensor exhibited significant saturation response. This response has two main features:

1) An optical effect due to stray light in the sensor that produces elevated digital counts preceding a saturated pixel, and
2) An electronic effect, e.g., bright target recovery (BTR), that produces elevated counts following a saturated pixel.

Furthermore, these effects are asymmetric with band number; even numbered bands exhibit greater stray light effects, while odd numbered bands exhibit greater bright target recovery effects. These effects were added to the simulated data to enhance realism. Using data from a sensor characterization examination in April 1993, methods were developed to simulate the stray light and BTR responses. Both are a function of the level of saturation, i.e., the real digital count value for a sensor not limited to 10-bit words. In the calculation discussed earlier, count values were saved as computed, i.e., not truncated to 10-bit accuracy as is the case for the actual flight.

The sensor characterization data provided the saturation responses at two levels of saturation, or overdrive, for each pixel in the scan line. A linear function was fit individually for each pixel away from the saturated pixel. This linear function fit provided an excellent reproduction of the tabulated saturation responses (Figs. 7 and 8).

3.7 Telemetry

The SeaStar data stream contains a large number of instrument and spacecraft telemetry fields in addition to the SeaWiFS science observations contained in the scan lines. These fields represent a combination of direct measurements from spacecraft hardware components, e.g., temperatures, voltages, and currents; status of commandable components, e.g., on or off, and A/B side switches, as well as tilt and gain settings; and computed values from onboard processors, e.g., spacecraft time, orbit position, and

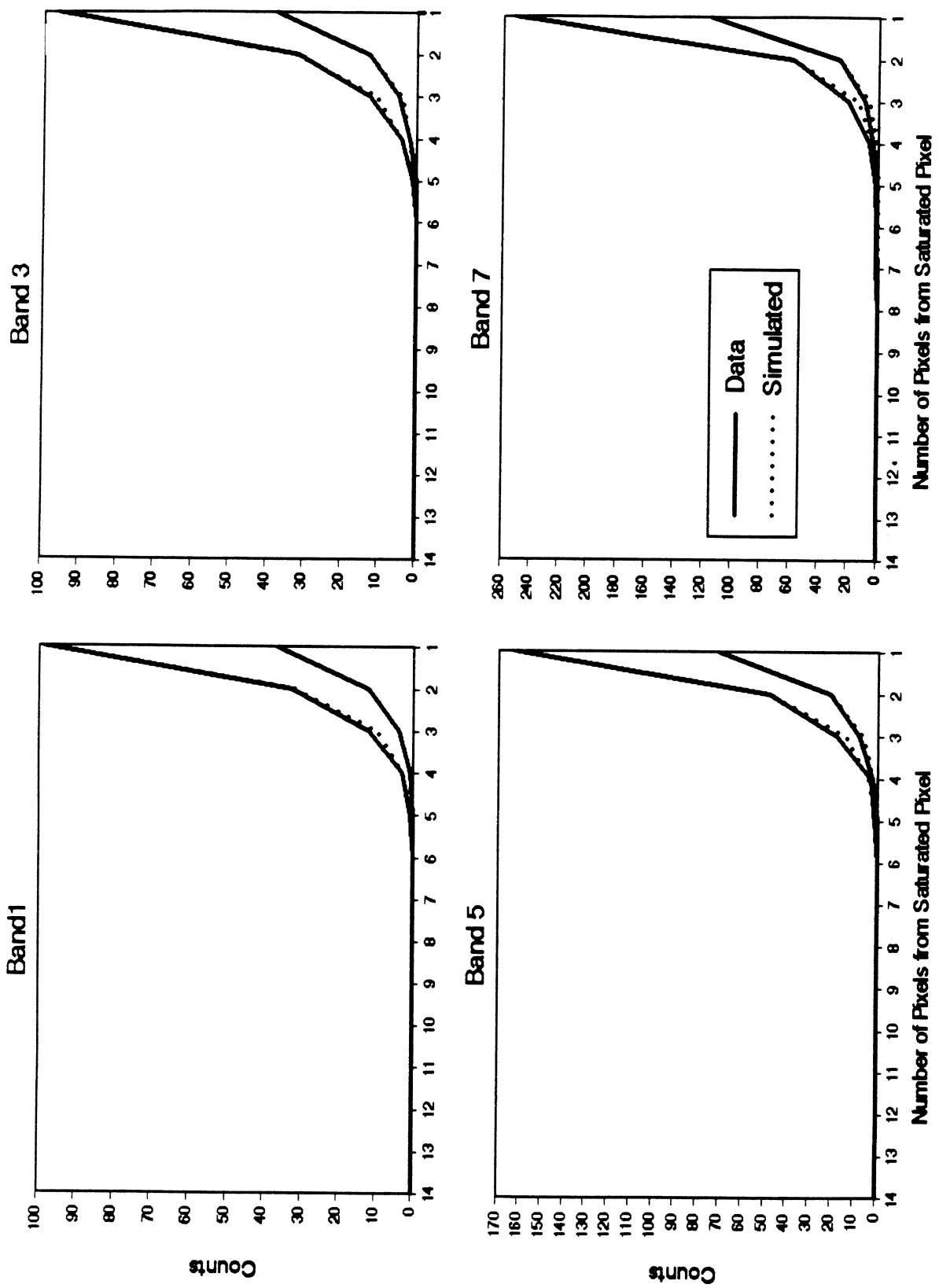

Fig. 7. Comparison of measured stray light response with computed response for odd-numbered bands. These bands exhibit the worst stray light response. This response is expected to improve significantly with sensor modifications.

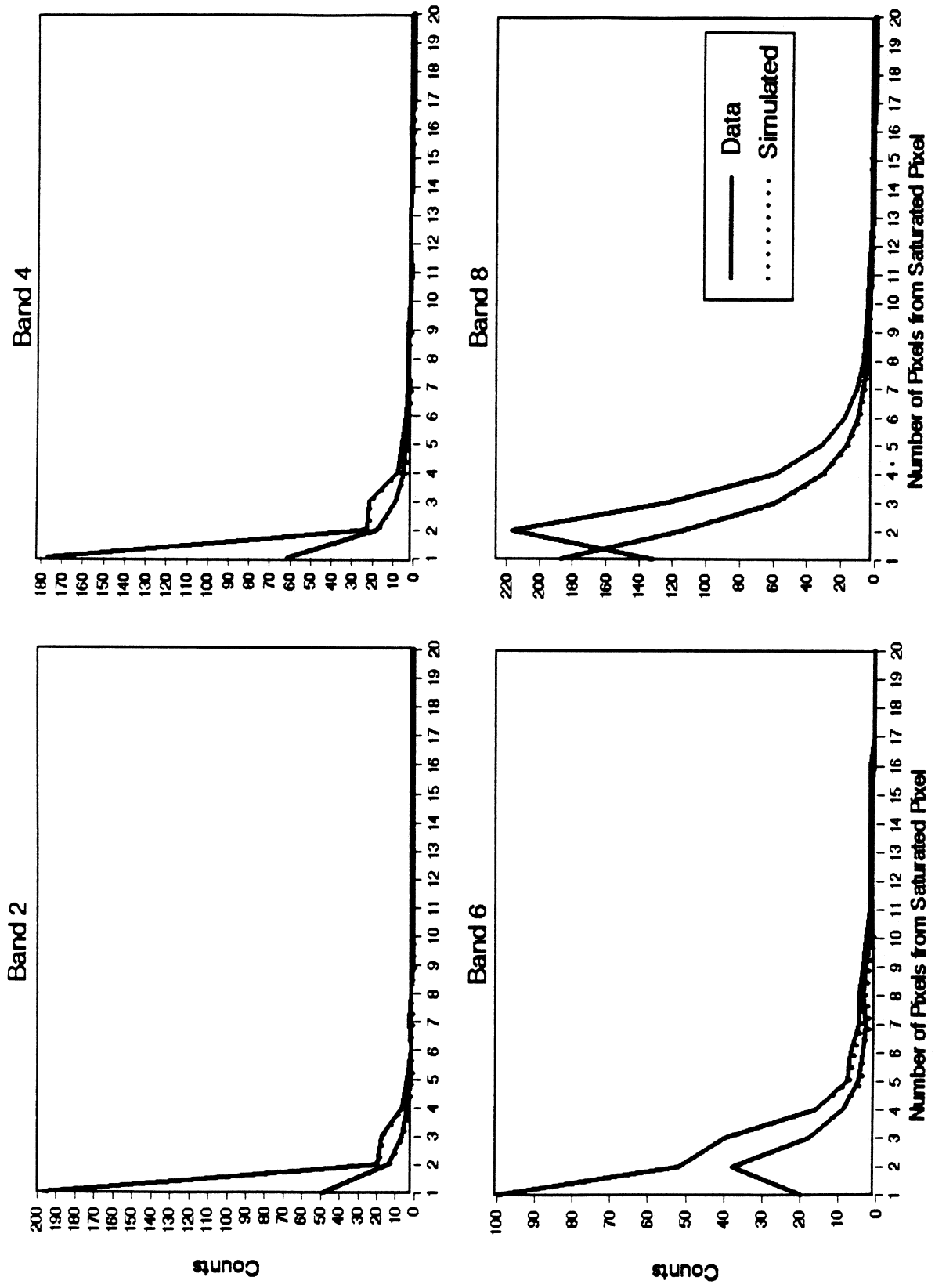

Fig. 8. Comparison of measured bright target recovery response with computed response for even-numbered bands. These bands exhibit the worst bright target recovery response. This response is expected to improve significantly with sensor modifications.

attitude. Fields that represent physical quantities (both measured and computed), also known as *analog* telemetry, are usually digitized for inclusion in the data stream, while status information, also known as *discrete,* is typically represented by single bit fields packed into status bits.

Several telemetry fields are required as input to the simulation process. They are:

a) scan line time,

b) orbit position and velocity,

c) spacecraft attitude,

d) instrument tilt angle (commanded and actual),

e) gain and TDI settings, and

f) instrument mode.

A number of additional fields are also included to support data processing and otherwise improve the realism of the data stream. Specific examples include instrument analog and digital telemetry, spacecraft attitude sensor data, and GPS telemetry. In addition, the spacecraft telemetry includes a large number of analog and status fields, from the attitude control system data, GPS subsystem, electrical power subsystem, propulsion subsystem, transmitters, and flight computers. In most cases, the information presently available for simulating these values is limited. The methods for each type of data are as follows.

The simulated science data discussed earlier are saved scan line-by-scan line. The scan line time and instrument mode are inserted for each LAC scan line and for every fifth GAC scan line, since GAC lines are stored five per minor frame (discussed in the next section). The gain and TDI are included with every scan line. Time, sensor tilt, and mode are required for the instrument telemetry packet, included for two of every three scan lines for both GAC and LAC. Time, orbit position and velocity, and spacecraft attitude are required for the ancillary data packet, included for one of every three scan lines. The remaining instrument telemetry fields are set to static values based on a sample of actual values provided by SBRC.

The spacecraft telemetry packet is included for 1 of every 3 scan lines for LAC data and 1 of 15 lines for GAC data, in accordance with the OSC specified onboard data structure. The scan line time, orbit, and attitude data for the appropriate scan line are included in the spacecraft telemetry. In addition, simulated attitude sensor data is generated for the spacecraft packet to support realistic navigation processing by the SDPS. The sensor data consist of sun angles and presence flags for each of three digital sun sensors, and Earth width and phase angles for each of two Earth scanners. The angles are computed using the simulated orbit and attitude data, according to the sensor manufacturer's specifications and information from OSC regarding the sensor mounting and orientation, as well as general reference information (Wertz 1978). The remaining spacecraft fields are set to arbitrary static values.

3.8 Data Formatting

The data is formatted according to the specifications provided by OSC for the SeaStar minor frame and the individual data packets. The LAC format is described in the *SeaStar Spacecraft L-band Downlink to Receiving Stations Interface Control Document (ICD),* currently being prepared by OSC. This document includes the overall minor frame format and details of the spacecraft identification (ID) and time tag, scan line data (including the gain and TDI), instrument telemetry, and ancillary data packets. However, the structure of the data fields is shown here for completeness (Fig. 9). The GAC minor frame format specifications were obtained from OSC, but are not yet available in a formal document. The formats of the GAC data ID, time tag, spacecraft telemetry packet, instrument telemetry packet and ancillary data packet are identical to the LAC data, although, the instrument and ancillary packets are stored in different locations in the GAC minor frame (Fig. 10). The GAC scan lines are formatted and stored according to the data reduction specifications provided by OSC.

The overall format of the LAC minor frame is given in Fig. 9, which shows the location of the major elements. As stored on the spacecraft, the data include a combination of 10-bit and 8-bit fields. All data, except the spacecraft telemetry, are stored as 10-bit words; the spacecraft fields are 8-bit aligned. The figure also shows a frame synch at the beginning of each minor frame and an auxiliary synch at the end; the simulation of these fields was not attempted, but will be added by the DCF to support end-to-end testing.

The Version 2 format is based upon this minor frame definition and on the initial frame formatting of the data. Clearly the 10-bit aligned data cannot be readily interpreted by standard computing systems. The DCF has provided a programmable frame formatter (PFF) which reformats the data into a more useful format. Specifically, each 10-bit word is right-justified in a 16-bit word, while the 8-bit words are maintained in their original format. The frame synchs are stripped and discarded. This processing increases the frame length from 13,860 bytes to 21,504 bytes, but greatly facilitates subsequent processing. The data in the format generated by the PFF is referred to as level-0, since it is the first format *seen* by the SDPS or any remote HRPT station.

The simulation reverses the processing performed by the DCF. First the simulated science and telemetry data are combined to generate a PFF (level-0) output file, with all data aligned in 16- or 8-bit fields. This format is not only much easier to generate initially, but also facilitates reading of the data by other software for quality control (QC); it can be ingested and processed directly by the SDPS for internal testing of its systems and all downstream functions (QC and data archiving).

The level-0 files are then processed to compress the 16-bit words to 10 bits to simulate the spacecraft format.

One Second of Real-Time Stream (Two Major Frames):

		<--6-->	<-2->	<-4->	<----620---->	<--44-->	<-8->	<----------10,304 Words---------->	<-2->	<--100-->
MF	mF 1	Frame Sync	S/C ID	Time Tag	S/C SOH TLM FIELD 1	Inst. TLM	Gn & TDI	One LAC Scan Line	20 bit pad	Auxiliary Sync
	mF 2	Frame Sync	S/C ID	Time Tag	S/C SOH TLM FIELD 2	Anc. TLM	Gn & TDI	One LAC Scan Line	20 bit pad	Auxiliary Sync
	mF 3	Frame Sync	S/C ID	Time Tag	S/C SOH TLM FIELD 3	Inst. TLM	Gn & TDI	One LAC Scan Line	20 bit pad	Auxiliary Sync
MF	mF 1	Frame Sync	S/C ID	Time Tag	S/C SOH TLM FIELD 1	Inst. TLM	Gn & TDI	One LAC Scan Line	20 bit pad	Auxiliary Sync
	mF 2	Frame Sync	S/C ID	Time Tag	S/C SOH TLM FIELD 2	Anc. TLM	Gn & TDI	One LAC Scan Line	20 bit pad	Auxiliary Sync
	mF 3	Frame Sync	S/C ID	Time Tag	S/C SOH TLM FIELD 3	Inst. TLM	Gn & TDI	One LAC Scan Line	20 bit pad	Auxiliary Sync
		<--15 Bytes-->			<----775---->	<55>	<10>	<----------12,880 Bytes---------->	<2.5>	<--125-->

White: 10-bit Telemetry Format
Dotted: 8-bit Telemetry Format

Note: **Minor frame is 11,090 10-bit words (13,860 bytes + 20 bit pad)**
Three minor frames per major frame
Two major frames per second

Words: **10 bit format (except shaded area)**
Bit 1 = MSB, Bit 10 = LSB
Bit 1 transmitted first

Fig. 9. SeaStar real-time telemetry format definition. *Inst. TLM* indicates instrument telemetry; *Anc. TLM* indicates ancillary telemetry. (Courtesy of Orbital Sciences Corporation).

GAC to LAC reduction ratio = 1:20
GAC minor frame produced every 3.33 seconds, major frame every 10 seconds

GAC:

		<--6-->	<-2->	<-4->	<---620--->	<-- 2016 -->	<-- 2016 -->	<-- 2016 -->	<-- 2016 -->	<-- 2016 -->	<--276 -->	<--100-->
MF	mF 1	Frame Sync	S/C ID	Time n	S/C SOH TLM FIELD 1	GAC Line n	GAC Line n+4	GAC Line n+8	GAC Line n+12	GAC Line n+16	Anc/Inst TLM	Auxiliary Sync
	mF 2	Frame Sync	S/C ID	Time n+20	S/C SOH TLM FIELD 3	GAC Line n+20	GAC Line n+24	GAC Line n+28	GAC Line n+32	GAC Line n+36	Anc/Inst TLM	Auxiliary Sync
	mF 3	Frame Sync	S/C ID	Time n+40	S/C SOH TLM FIELD 2	GAC Line n+40	GAC Line n+44	GAC Line n+48	GAC Line n+52	GAC Line n+56	Anc/Inst TLM	Auxiliary Sync
		<----15 Bytes--->			<----775---->	<-- 2520 -->	<-- 2520 -->	<-- 2520 -->	<-- 2520 -->	<-- 2520 -->	<-- 345 -->	<--125 -->

LAC:

		<-6->	<-2->	<-4->	<---620--->	<-- 44 -->	<---------- 10,312 ---------->	<--100-->
MF	mF 1	Frame Sync	S/C ID	Time Tag	S/C SOH TLM FIELD 1	Inst. TLM	Stored LAC Line (including Gn & TDI Pixel) n	Auxiliary Sync
	mF 2	Frame Sync	S/C ID	Time Tag	S/C SOH TLM FIELD 2	Anc. TLM	Stored LAC Line (including Gn & TDI Pixel) n+1	Auxiliary Sync
	mF 3	Frame Sync	S/C ID	Time Tag	S/C SOH TLM FIELD 3	Inst. TLM	Stored LAC Line (including Gn & TDI Pixel) n+2	Auxiliary Sync
		<---15 Bytes--->			<----775---->	<-- 55 -->	<---------- 12,890 ---------->	<--125-->

White: 10-bit Telemetry Format
Dotted: 8-bit Telemetry Format

Revision: 9
Date: 4/13/93

Note: **Stored LAC/GAC Minor Frame Length is 11,088 10-bit Words (13,860 Bytes)**
Three Minor Frames Per Major Frame
Stored LAC/GAC downlinked on S-Band at 2.0 Mbps using HDLC packet structure

10 bit format (except shaded areas)
Bit 1 = MSB, Bit 10 = LSB
Bit 1 transmitted first

Fig. 10. SeaStar stored telemetry format definition. (Courtesy Orbital Sciences Corporation).

Table 12. SeaStar spacecraft telemetry engineering conversion of analog telemetry.

Analog Telemetry Points	*Units*	*Start Byte*	*Byte Length*	*Slope*	*Intercept*
Orbit X position (ECEF)	m	143	4	0.00391155	−8400000.0
Orbit Y position (ECEF)	m	147	4	0.00391155	−8400000.0
Orbit Z position (ECEF)	m	151	4	0.00391155	−8400000.0
Orbit X velocity (ECEF)	$\mathrm{m\,s^{-1}}$	155	4	3.49246E-6	−7500.0
Orbit Y velocity (ECEF)	$\mathrm{m\,s^{-1}}$	159	4	3.49246E-6	−7500.0
Orbit Z velocity (ECEF)	$\mathrm{m\,s^{-1}}$	163	4	3.49246E-6	−7500.0
Attitude yaw angle	degrees	121	2	0.00549316	−180.0
Attitude roll angle	degrees	123	2	0.00549316	−180.0
Attitude pitch angle	degrees	125	2	0.00549316	−180.0
Sun sensor 1 angle 1	degrees	61	2	0.001953125	−64.0
Sun sensor 1 angle 2	degrees	63	2	0.001953125	−64.0
Sun sensor 2 angle 1	degrees	67	2	0.001953125	−64.0
Sun sensor 2 angle 2	degrees	69	2	0.001953125	−64.0
Sun sensor 3 angle 1	degrees	73	2	0.001953125	−64.0
Sun sensor 3 angle 2	degrees	75	2	0.001953125	−64.0
Earth scanner 1 phase	degrees	79	2	0.005493164	0.0
Earth scanner 1 width	degrees	81	2	0.005493164	0.0
Earth scanner 2 phase	degrees	85	2	0.005493164	0.0
Earth scanner 2 width	degrees	87	2	0.005493164	0.0

ECEF = Earth-Centered Earth-Fixed

Place holders are inserted for the frame synch words to be filled by the DCF. These files are then used by the DCF and the GSFC Code 500 Simulation Operations Center (SOC) to generate simulated data tapes which can be used to test the WFF data receipt, transmission to GSFC, and PFF processing. A description of the DCF and SOC simulation support is beyond the scope of this paper. All of the scan lines and telemetry corresponding to each data collection period are collected and formatted as a unit. The methods involved in formatting the individual fields and packets for the minor frames are different for each type of data and are as follows. The spacecraft ID is computed for each minor frame from the frame number and the data type. As shown in Fig. 9, there are three minor frames per major frame; the frame number is started at 1 at the beginning of each data collection period and cycled for all frames in the period. The time tag is converted to two integer fields corresponding to the truncated Julian day (days since 13 January 1993, at midnight GMT, Julian day 2,449,000.5) and the milliseconds of the day; the significant bits of these two fields are combined into a 40-bit time tag, which is divided into four 10-bit words.

The spacecraft telemetry fields are digitized and stored according to the best available specifications from OSC (Table 12). *Note that these specifications have not been updated since September 1992 and are very likely to change prior to launch.* Spacecraft fields are included only for the first minor frame of each major frame, corresponding to spacecraft (S/C) state of health (SOH) telemetry, (field 1 in Fig. 9). OSC has designated fields 2 and 3 as dynamic and are therefore, not useful for data processing. All fields are digitized using a linear conversion (with a specified slope and offset) and stored in either 16 or 32 bits. The remaining spacecraft packet bytes are set to arbitrary values (determined as the byte offset modulo 256).

The instrument telemetry specifications are shown in Table 13. Note that, although the instrument data are included in the 10-bit portion of the minor frame, in fact only the 8 least significant bits (LSB) of each word are used. The instrument analog telemetry fields also use linear digitization specifications. The measured tilt angle is the only actively simulated analog value. The tilt alignment status and the sensor mode (Earth or solar) are used to set the appropriate discrete status bits; the mirror side bit is alternated for the LAC scan lines. The time tag is set to the milliseconds since the last exact second. The remaining fields are set to fixed, but realistic, values as stated above.

The ancillary data specifications are shown in Table 14. The ancillary data fields use signed integers rather than linear conversions for digitization; the units are meters and meters per second for the orbit data, and microradians for the attitude angles. The time tag is set to the milliseconds-of-day.

The gain and TDI for each band are combined into a single 10-bit field, with the 8 fields corresponding to the 8 bands immediately preceding each scan line in the minor frame, as shown in Fig. 9. (Note that the gain values in the data are 0 through 3, corresponding to gains 1 through 4 in Table 5.) Each scan line is also preceded in the frame

Table 13. SeaStar instrument telemetry specification.

Word Number	*Bit Number*	*Time Stamp of Sync Pulse in Scan Line*
1		Milliseconds Since Last GPS Pulse
2		Milliseconds Since Last GPS Pulse
3		Milliseconds Since Last GPS Pulse
4		Milliseconds Since Last GPS Pulse
Word No.	*Bit No.*	*SeaWiFS Discrete Telemetry*
5	1	Pad
5	2	Pad
5	3	Servo A or B Select
5	4	AMC On[1]
5	5	Servo A Locked
5	6	Servo B Locked
5	7	Timing A or B Select
5	8	Tilt A On
5	9	Tilt B On
5	10	Tilt Telemetry On
6	1	Pad
6	2	Pad
6	3	Stow On
6	4	Stow Aligned
6	5	Heaters Enable
6	6	Solar Door Status
6	7	Analog Power On
6	8	Tilt Platform Limit
6	9	Tilt Base Limit
6	10	Tilt Nadir (0°) Aligned
7	1	Pad
7	2	Pad
7	3	Tilt Aft (+20°) Aligned
7	4	Tilt Forward (−20°) Aligned
7	5	Data Mode Select
7	6	Half Angle Mirror Side
7	7	Image Data Sync
7	8	AMC at Speed
7	9	AMC at Speed
7	10	Spare

Word Number	*SeaWiFS Analog Telemetry*
8	Band 1 and 2 FPA Temperature[2]
9	Band 3 and 4 FPA Temperature
10	Band 5 and 6 FPA Temperature
11	Band 7 and 8 FPA Temperature
12	Telescope Motor Temperature
13	Tilt Base Temperature
14	Tilt Platform Temperature
15	Half Angle Motor Temperature
16	Power Supply A Input Current
17	Power Supply B Input Current
18	+15 V Analog Power Voltage
19	−15 V Analog Power Voltage
20	+5 V Logic Power Voltage
21	Power Supply Temperature
22	B1 and B2 Post-amplifier Temperature
23	Servo Driver Temperature
24	+30 V Servo Power Voltage
25	+21 V Servo Power Voltage
26	−21 V Servo Power Voltage
27	+5 V Servo Power Voltage
28	AMC Phase Error
29	Tilt Platform Position
30	Tilt Base Position
31	+28V Heater Power
32	Telescope A Motor Current
33	Telescope B Motor Current
34	Half-Angle Mirror A Motor Current
35	Half-Angle Mirror B Motor Current
36	Servo A Phase Error
37	Servo B Phase Error
38	AMC A Motor Current
39	AMC B Motor Current
Word No.	*Padding to Fill 44 Word Field*
40	Spare
41	Spare
42	Spare
43	Spare
44	Spare

AMC = Angular Momentum Compensation
FPA = Focal Point Assembly

by *start synch* and *dark restore* pixels, and followed by a *stop synch* pixel. Thus, the total number of stored pixels per scan line is three more than the actual number of data pixels (1,288 for LAC and 251 for GAC). The start and stop synchs are set to alternating values of 0 and 1,023 (10 binary ones) based on information provided by OSC, while the dark restore value is arbitrarily set to 20 for all bands.

The scan line radiances are initially computed using the full 16-bit dynamic range, to allow realistic computation of the sensor saturation response. The final step prior to inclusion in the minor frame is to truncate all values to 1,023 (maximum 10-bit value). The completed minor frame is then written to the level-0 simulated data file.

4. EXAMPLES OF DATA

This section includes examples of GAC, stored LAC, and real-time HRPT data.

4.1 GAC Data

Simulated Version 2 data for SeaWiFS band 1 for the second (daytime) downlink on 25 March 1994, mapped to Earth coordinates, shows how the descending node orbit acquires GAC data (Fig. 11). This image shows eight full descending nodes of data, plus a partial node over Wallops prior to a daytime downlink (the Wallops visibility mask is illustrated). Approximately half of an overpass at Wallops results in downlinked data for that opportunity since the spacecraft contains two onboard data recorders—one transmits while the other acquires. The remaining half of the data taken during the overpass will be received at the next (night) downlink.

In Fig. 11, the grey scale shows lower (darker) to higher (lighter) count values representing total, at-satellite radiances. White indicates saturation; in this case, due almost entirely to clouds and ice. (See also Plate 1, where a blue-to-green-to-red scale is used, and the brightest red indicates saturation.) Some saturated pixels, however, may be noted in the Saharan Desert. Note that even clouds and ice do not saturate at higher latitudes due to reduced incident irradiance. The *pinching* of the swath width near the equator shows the effects of the tilt change. The tilt change requires the sensor to pass through nadir, where the swath width is reduced relative to tilted scans. The black speckles in this region indicate lost coverage due to excessively large effective ground speed, a function of the orbital speed and the tilt change speed (see Fig. 1). It is not clear how well data collected during a tilt change will be navigated due to attitude perturbations resulting from the tilt motor. In this simulated data set, no such perturbations were allowed to occur and pointing information is as well known as anywhere in the orbit. Other than navigation difficulties and a large occurrence of sun glint, data collected during a tilt change is expected to be of high scientific quality.

Whereas band 1 saturates only over clouds, ice, and parts of the Saharan Desert, band 8 saturates over nearly all land features (Fig. 12; Plate 1). This is because vegetated areas have large reflectance in the near-infrared regions of the solar spectrum (Fig. 6).

A relatively cloud-free portion of a GAC orbit was selected to show how GAC data will actually look, as received, in the data stream. A section for band 1 shows Haiti and the Dominican Republic—near the center of the image—as dark, with Puerto Rico slightly to the east (Fig. 13; Plate 2). Greater variability is seen over the land than over the oceans. This is because ocean at-satellite radiances are dominated by the atmosphere (approximately 90% of the total), and in particular, Rayleigh scattering. Some minor brightening may be seen near the scan edges due to increased Rayleigh scattering as a function of the greater atmospheric path length here.

An image of band 8 shows land as saturated once again (Fig. 14; Plate 2). The blocky, rectangular features now

Table 14. SeaStar ancillary telemetry specification.

Word No.	*Time Reference*
1	Milliseconds since Midnight UTC (MSB first)
2	Milliseconds since Midnight UTC
3	Milliseconds since Midnight UTC
4	Milliseconds since Midnight UTC (LSB last)
Word No.	*Orbit Position Data*[1]
5	X (MSB first)[2]
6	X
7	X
8	X (LSB last)
9	Y (MSB first)
10	Y
11	Y
12	Y (LSB last)
13	Z (MSB first)
14	Z
15	Z
16	Z (LSB last)
Word No.	*Orbit Velocity Data*[3]
17	$\dot{X}$ (MSB first)
18	$\dot{X}$ (LSB last)
19	$\dot{Y}$ (MSB first)
20	$\dot{Y}$ (LSB last)
21	$\dot{Z}$ (MSB first)
22	$\dot{Z}$ (LSB last)
Word No.	*Attitude Angular Position Data*[4]
23	Φ (MSB first)
24	Φ (LSB last)
25	θ (MSB first)
26	θ (LSB last)
27	Ψ (MSB first)
28	Ψ (LSB last)
Word No.	*Attitude Angular Rates Data*[5]
29	$\dot{\Phi}$ (MSB first)
30	$\dot{\Phi}$ (LSB last)
31	$\dot{\theta}$ (MSB first)
32	$\dot{\theta}$ (LSB last)
33	$\dot{\Psi}$ (MSB first)
34	$\dot{\Psi}$ (LSB last)
35–44	Spare

1. ECEF Cartesian, units are in meters.
2. MSB is the acronym for *most significant bits*.
3. ECEF Cartesian, units are in $\mathrm{m\,s^{-1}}$.
4. Spacecraft centered coordinate system of roll and pitch (Φ and θ, respectively), and yaw (Ψ); all of the units are in μrad.
5. Spacecraft centered coordinate system of roll and pitch (Φ and θ, respectively), and yaw (Ψ); all of the units are in $\mu\mathrm{rad\,s^{-1}}$.

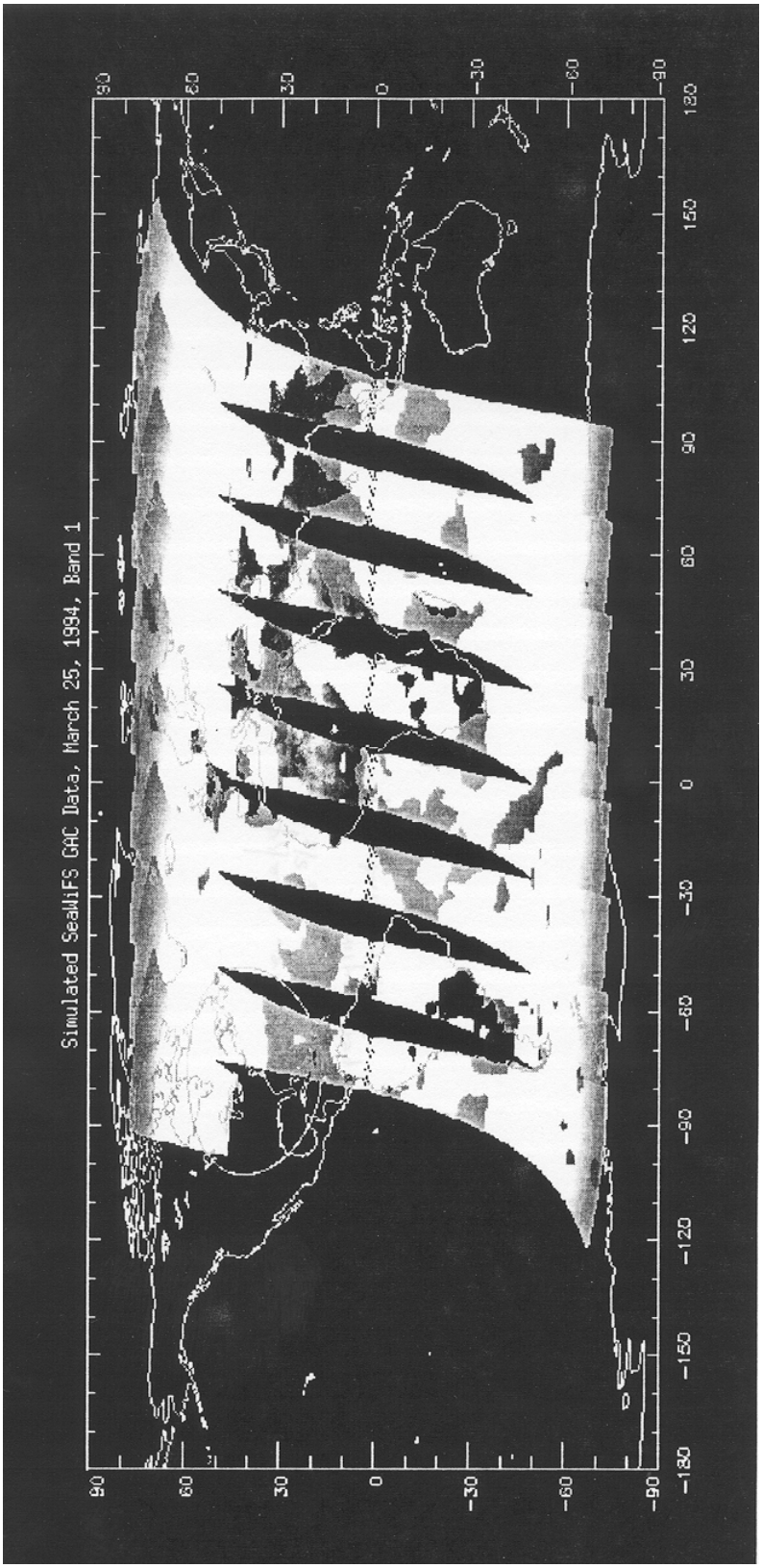

Fig. 11. Version 2 simulated SeaWiFS GAC data, 25 March 1994, band 1, mapped to Earth coordinates.

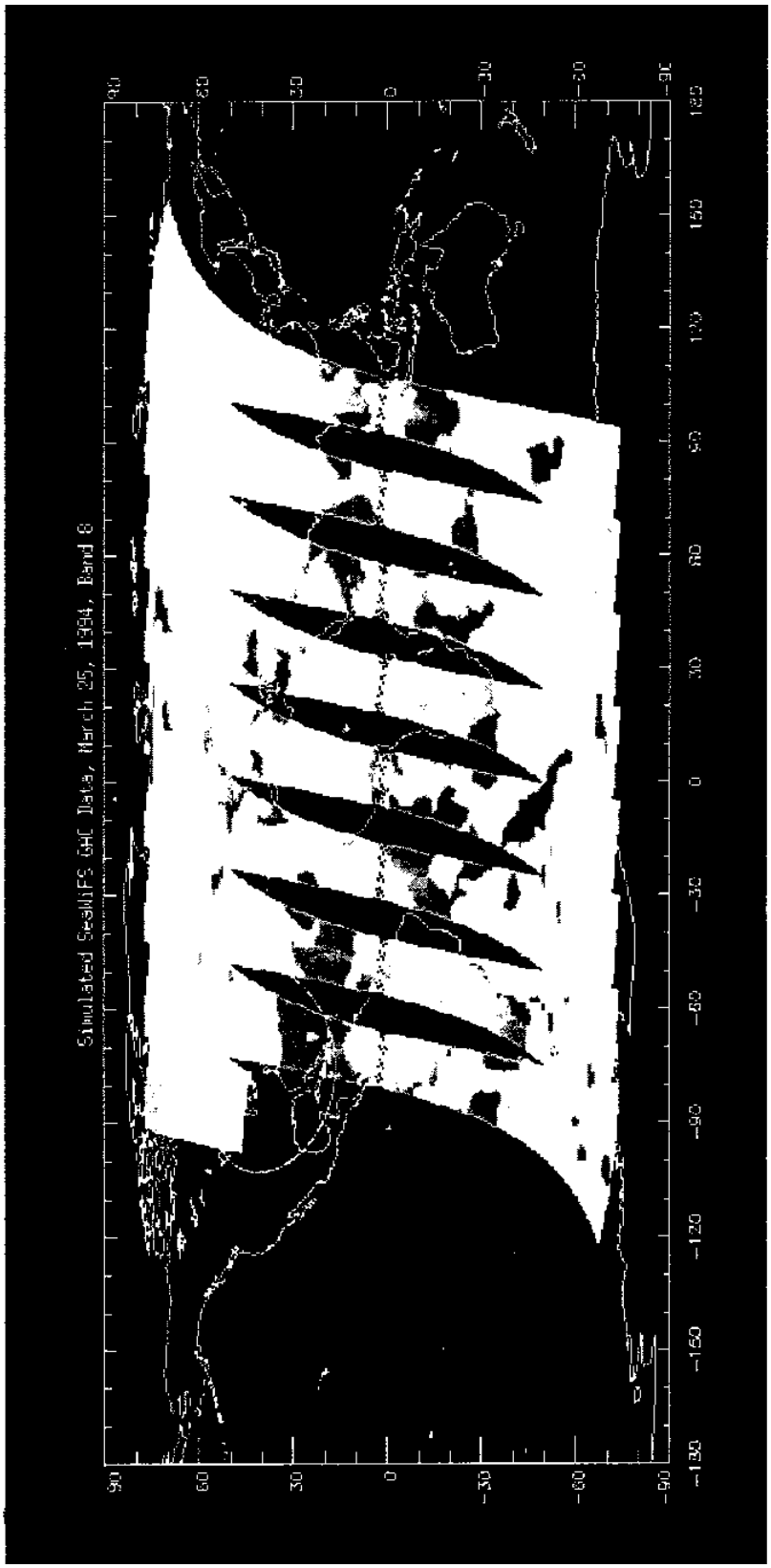

Fig. 12. Version 2 simulated SeaWiFS GAC data, 25 March 1994, band 8, mapped to Earth coordinates.

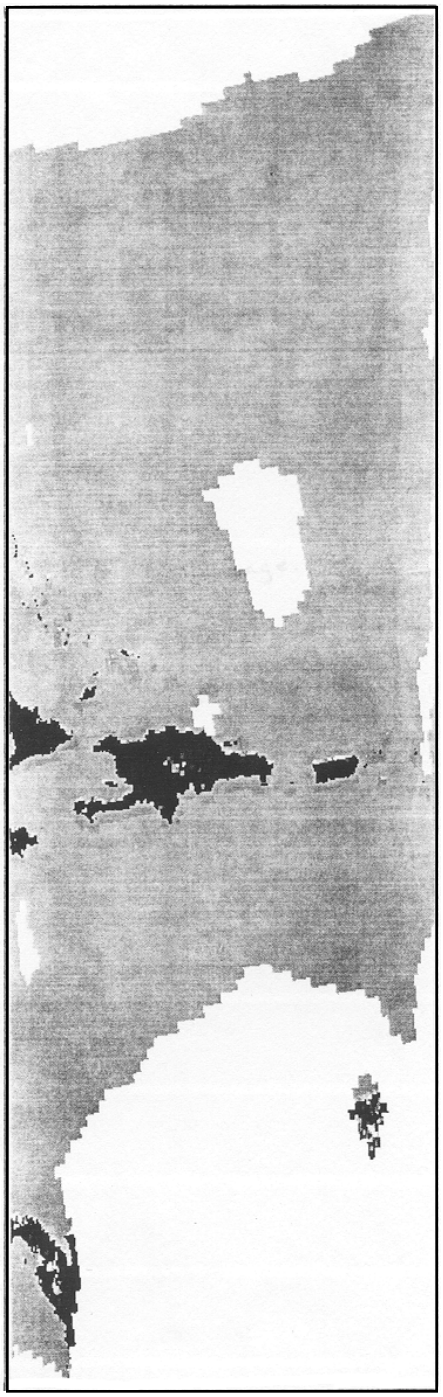

Fig. 13. A portion of Version 2 simulated SeaWiFS GAC data, band 1, in satellite coordinates (i.e., scan is x axis, orbit propagation direction is y axis). The Dominican Republic and Haiti is the dark object near the center of the image, with Puerto Rico just to the east. The grey scale indicates low at-satellite radiance (dark) to high radiance (bright). All of the bright white objects in this image are clouds.

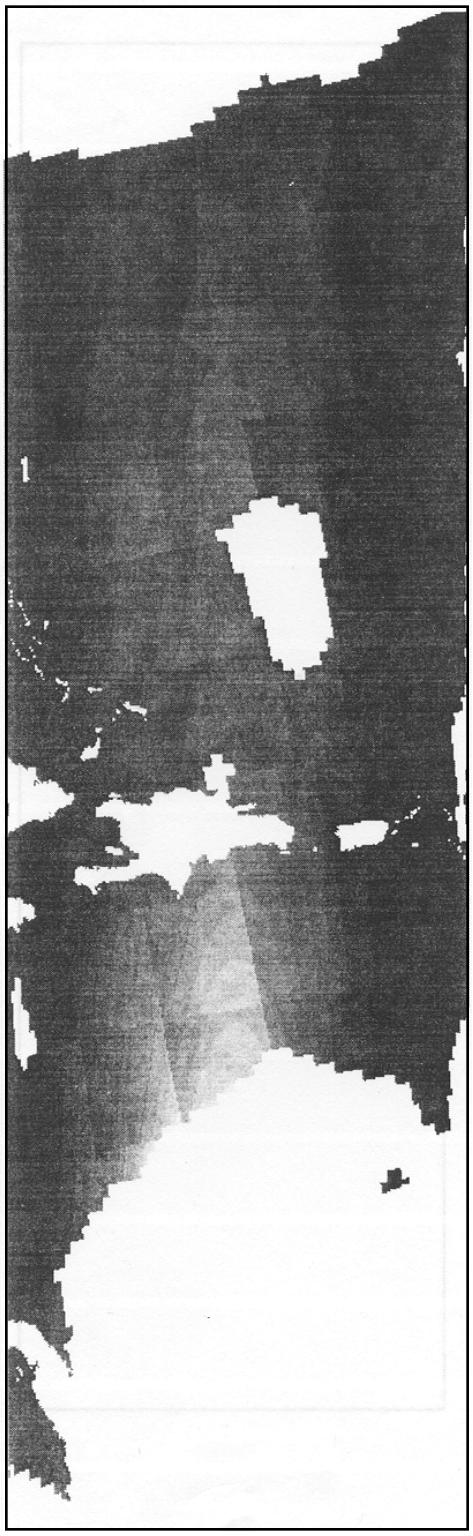

Fig. 14. As in Fig. 13 but for band 8. Land features are saturated in band 8.

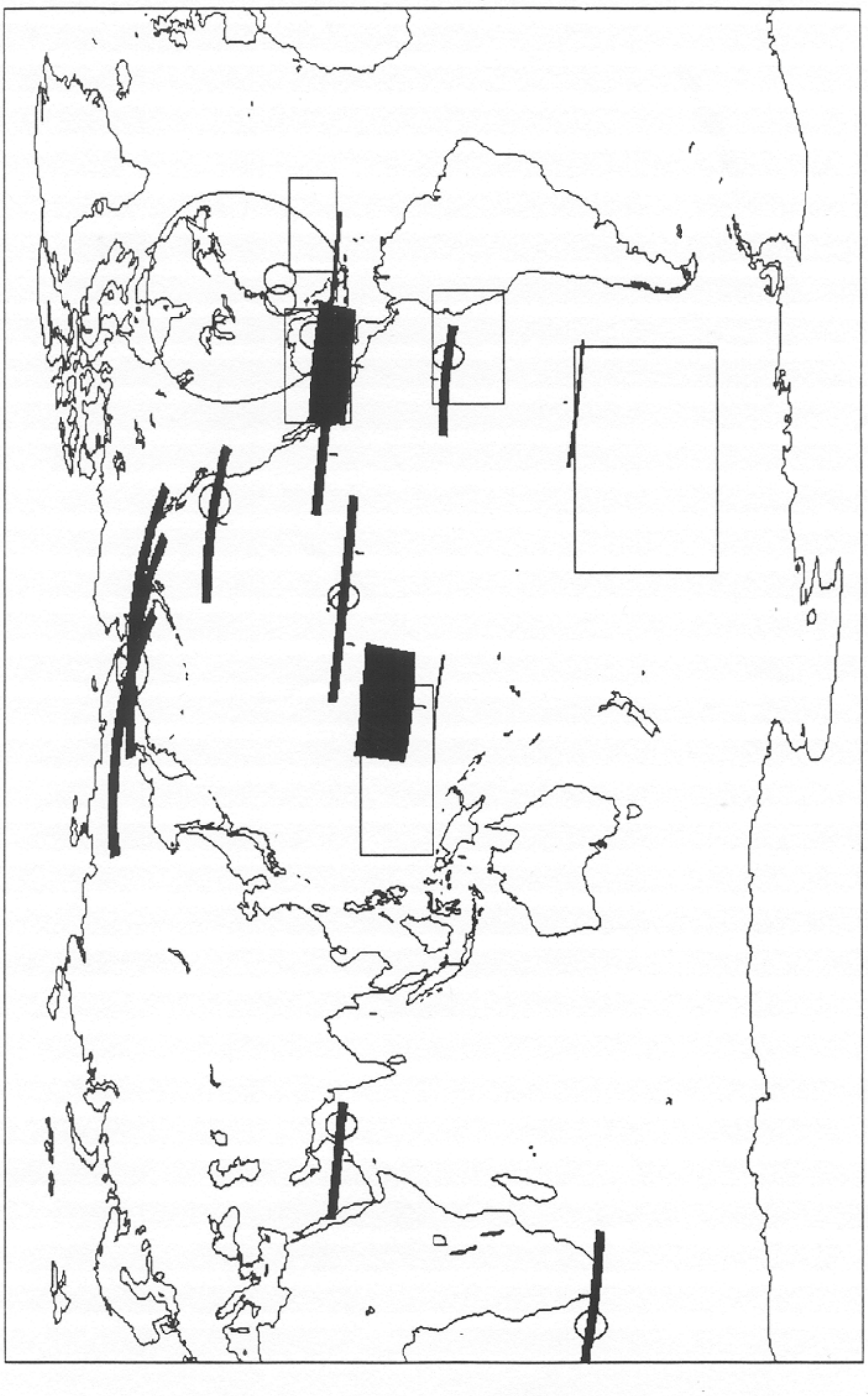

Fig. 15. *In situ* targets scheduled for 25 March 1994. Ship and buoy targets are denoted by circles, region targets by squares.

visible, are the result of the coarse resolution wind speed and pressure fields used to compute aerosol and sun glint, and Rayleigh scattering contributions, respectively. Some evidence of minor sun glint contamination may be seen in the southern portion of the image, near the center, before obscuration by clouds. Because of the small saturation radiance in band 8 (see Table 10), this band is particularly subject to sun glint contamination, even though greater values occur at other bands.

4.2 Stored LAC Data

Stored LAC data collection in the simulated data set follows the command schedule described earlier. The *in situ* target data acquisition schedule for 25 March 1994, is shown in Fig. 15. Simulated LAC data for the second (daytime) downlink on 25 March conform to three of the *in situ* target sites (Fig. 16). Many of the other target sites are included in the first (nighttime) downlink on 26 March 1994 (Fig. 17), although they appear in the schedule for March 25 because actual data collection occurs at this time. The remaining targets in the 25 March schedule are downlinked at the next Wallops overpass. This scenario illustrates the difficulties in creating schedule data that occur on GMT boundaries and data collection which is tied to local noon and midnight Wallops overpasses.

Actual images of the first three LAC segments in band 1 show the high spatial resolution of LAC data (Fig. 18; Plate 3). The first segment occurs over Saudi Arabia, and the second over South Africa, and the third over Cuba (Fig. 19), in a similar view of the GAC image shown earlier (Fig. 13), but exhibiting the larger swath width of LAC data. Note that the saturation at the scan edges on all three segments is due to the very large atmospheric path length (nearly 72° spacecraft zenith angle tilted) in this Version 2 data. A solar calibration with an intergain check is also included in the LAC data on each day of the simulated data set. A depiction of solar calibration and intergain check LAC data is shown in Fig. 20. Recall that the procedure involved acquiring data in solar mode off the solar diffuser at specified gains first, followed by intergain checks using the so-called calibration pulse. The truncated object on the left represents the solar calibration data, while the perpendicular stripe represents the results of the calibration pulse, which is solid in color until completion of the solar calibration. Then the intergain check begins, represented by alternating bands of six scans at selected gains.

The TDI check is similar to the solar calibration activity, but is shorter in duration (Fig. 21). Although solar diffuser data appear brighter in the center, they are not in this simulation. The increased brightness is due to different grey scaling given the absence of the intergain check. Data from different detector combinations are assumed to be identical in this simulated set.

A full moon occurs during the period of the simulated data set. The required 7° phase angle for data acquisition actually occurs in the GMT morning of 27 March 1994. Simulation of the lunar calibration uses data collected from an actual scan of the full moon from the SeaWiFS sensor in December 1992. These data produced the image shown in Fig. 22. For the simulated data set, the actual moon data were packaged into a realistic scan of two minutes in duration, showing the actual size of the moon within the downlinked SeaWiFS scan data (Fig. 23).

4.3 Real-Time HRPT Data

Simulated data acquired at the GSFC HRPT station are also provided in this data set. Mapped to Earth coordinates, a single overpass of SeaStar at the GSFC station appears as in Fig. 24, where the GSFC visibility mask is denoted. This overpass is band 1, and is the first pass of 25 March 1994. Thus, the pass may be related to the corresponding GAC image (Fig. 11). Note that the data collection does not obey the GSFC station mask boundaries. This is a result of the fact that the sensor is tilted aft of the velocity vector at this location, and the fact that the sensor scans 58° west-to-east of the satellite position.

A non-mapped view of Version 2 simulated real-time HRPT data is provided for band 1 in Fig. 25 (also Plate 4). The Florida peninsula is visible at the western edge of the scan, with Cuba, Haiti, and the Dominican Republic, and Puerto Rico successively west-to-east along the southern portion of the image. One may note significant saturation along the extreme western edge of the scans. This image corresponds directly with the GAC image shown earlier (Fig. 13), as well as with the third recorded LAC segment shown in Fig. 19. This sequence of images shows the relationships among GAC data, stored LAC data, and real-time HRPT data.

Version 2 HRPT data for band 8 shows once again that land saturates at this wavelength (Fig. 26; Plate 5). What is particularly notable is the high resolution of land features, resulting from the use of the high resolution WVS land mask.

4.4 Version 2 Sensor Saturation Response

The April 1993 sensor saturation response is fairly subtle and consequently is not readily apparent in the images discussed up to now. A close-up view is provided here of a portion of an HRPT image to illustrate the saturation response effects. The image portion chosen is a segment on the east coast of Puerto Rico, where a number of saturating islands and coastlines occur. Band 8 was chosen because it saturates over these land features (bands 1–5 most likely will not saturate here). The evidence is again somewhat subtle, but saturation effects appear as a kind of *blurring* preceding (stray light effects) and following (bright target recovery effects) small land objects (Fig. 27; Plate 6).

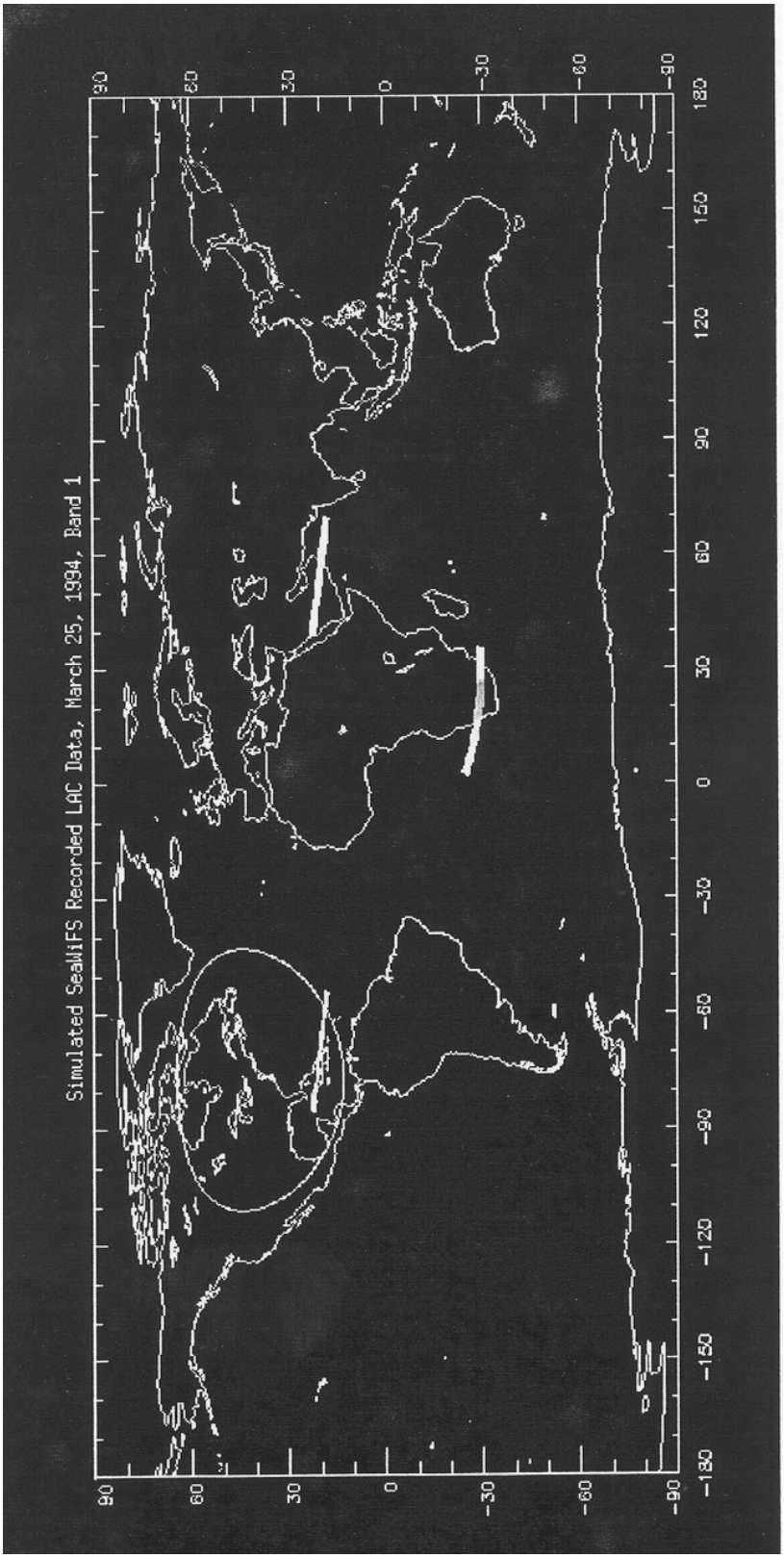

Fig. 16. Three recorded Version 2 LAC segments for March 25, 1994, mapped to Earth coordinates. The segments correspond to part of the schedule shown in Fig. 15.

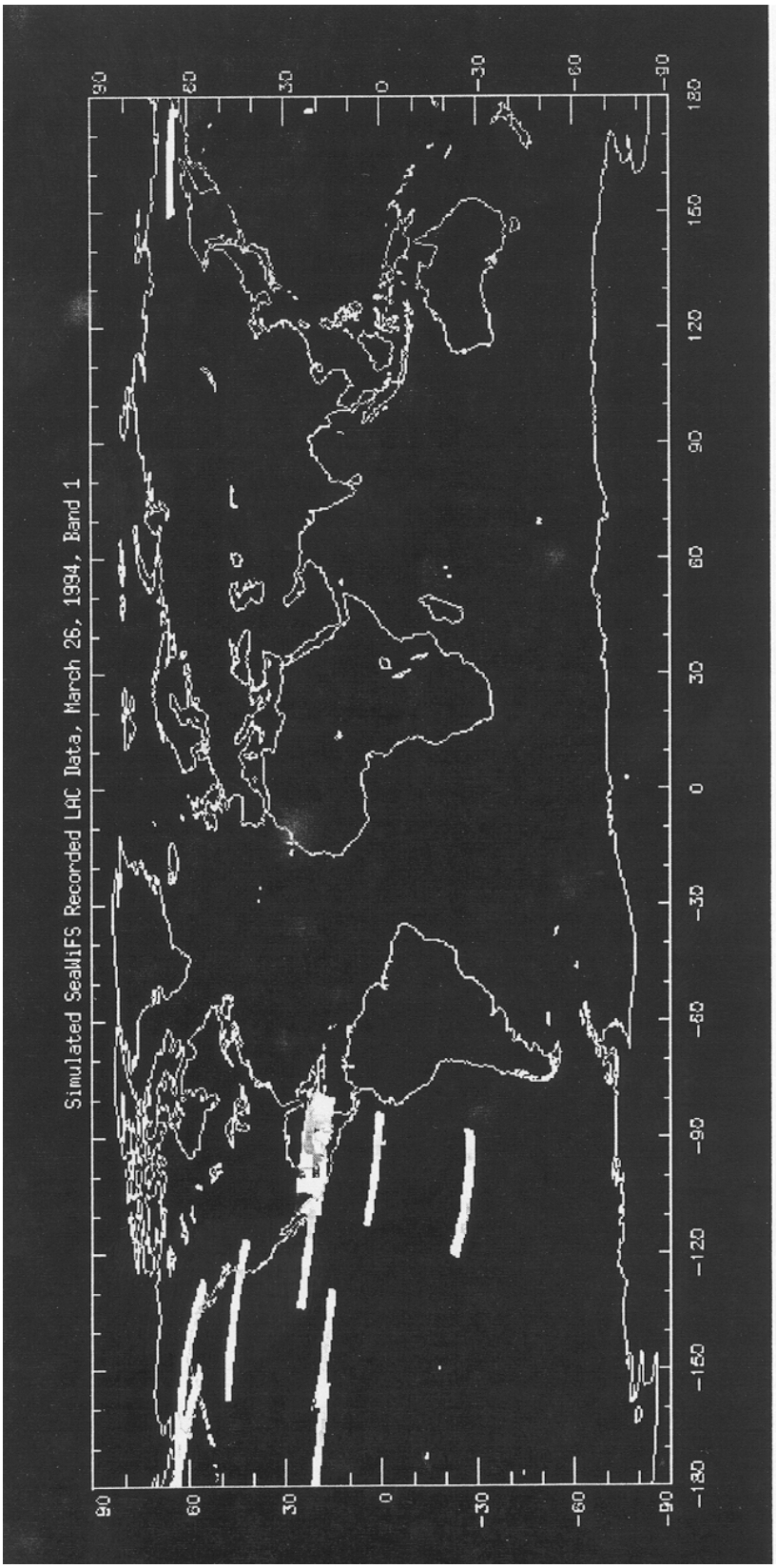

Fig. 17. Version 2 recorded LAC segments for the first downlink on March 26, 1994. These segments appeared on the schedule for March 25, but are not acquired on the ground until the local midnight pass on March 26.

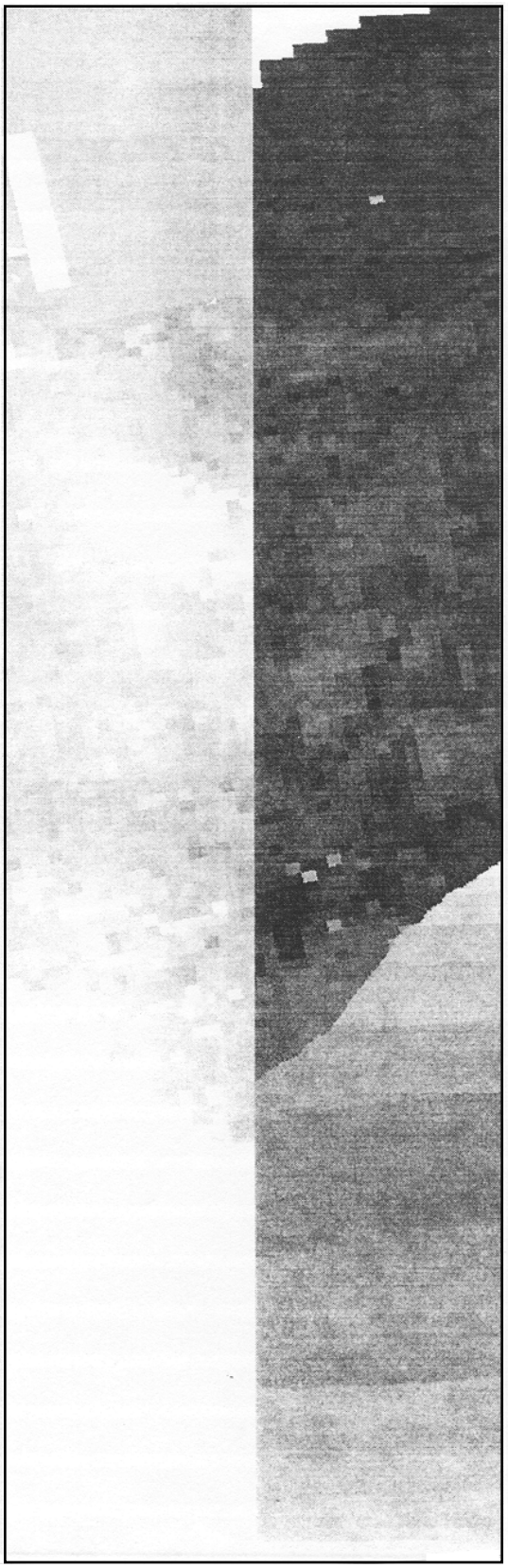

Fig. 18. Two of the recorded LAC segments shown in Fig. 16, of band 1, in satellite coordinates. The first segment is over Saudi Arabia, and the second over South Africa.

Fig. 19. The third LAC segment from Fig. 16, showing Cuba at the extreme western edge.

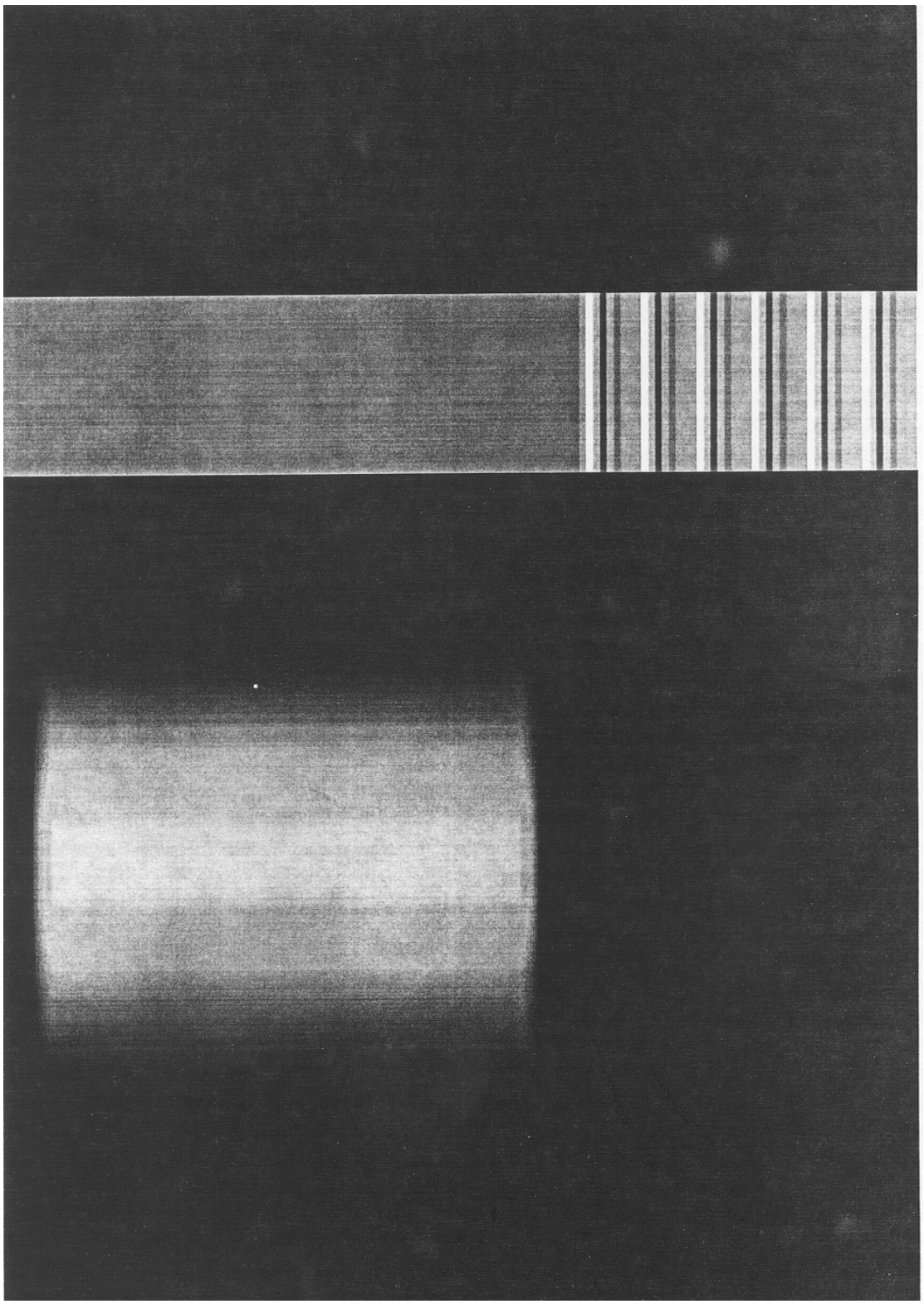

Fig. 20. Solar calibration/intergain check sequence. The solar calibration (consisting of observations of radiance reflected off the solar diffuser plate) is at the upper left, and the stripe extending the length of the page are the retrievals from the calibration pulse. Where the stripe shows alternating magnitudes is where the intergain check occurs.

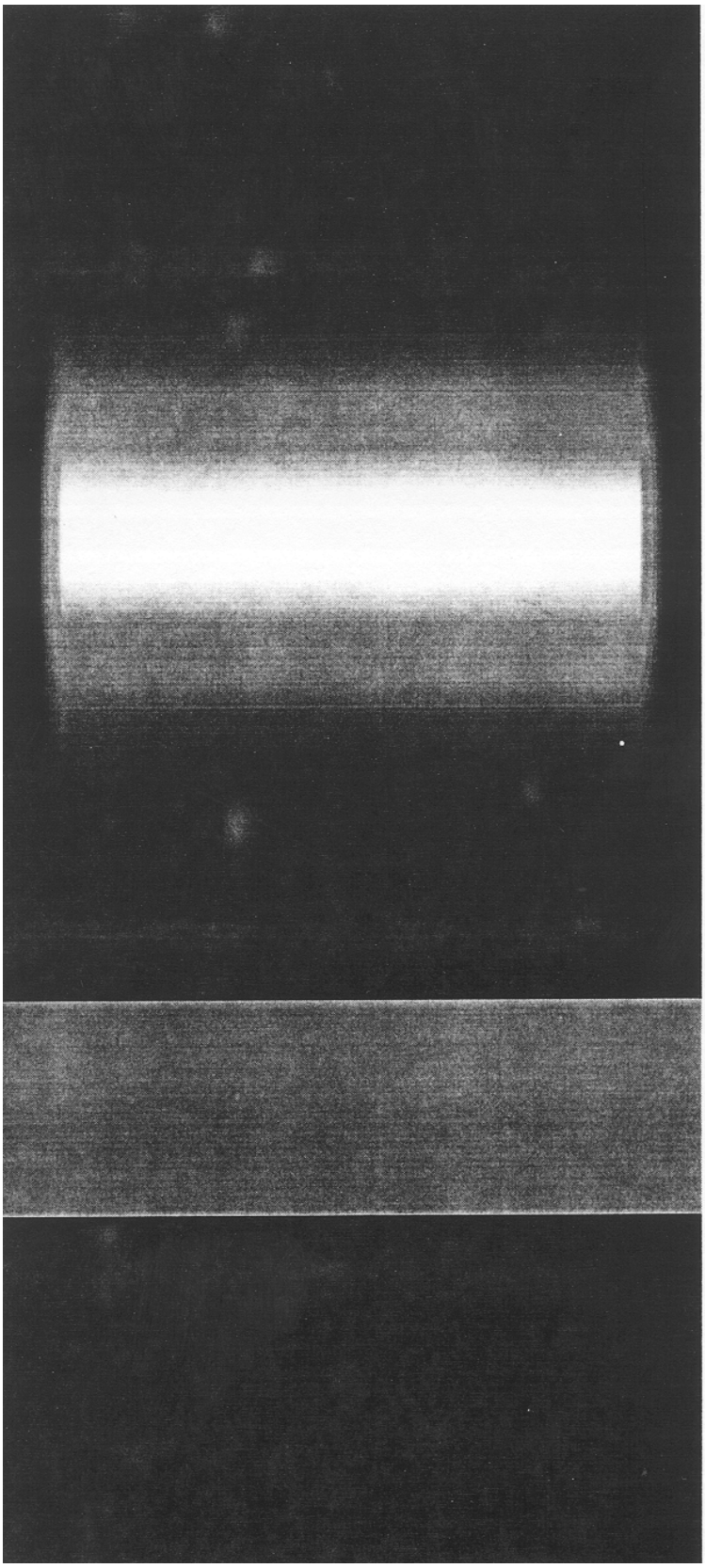

Fig. 21. TDI check sequence. This activity also uses the solar diffuser.

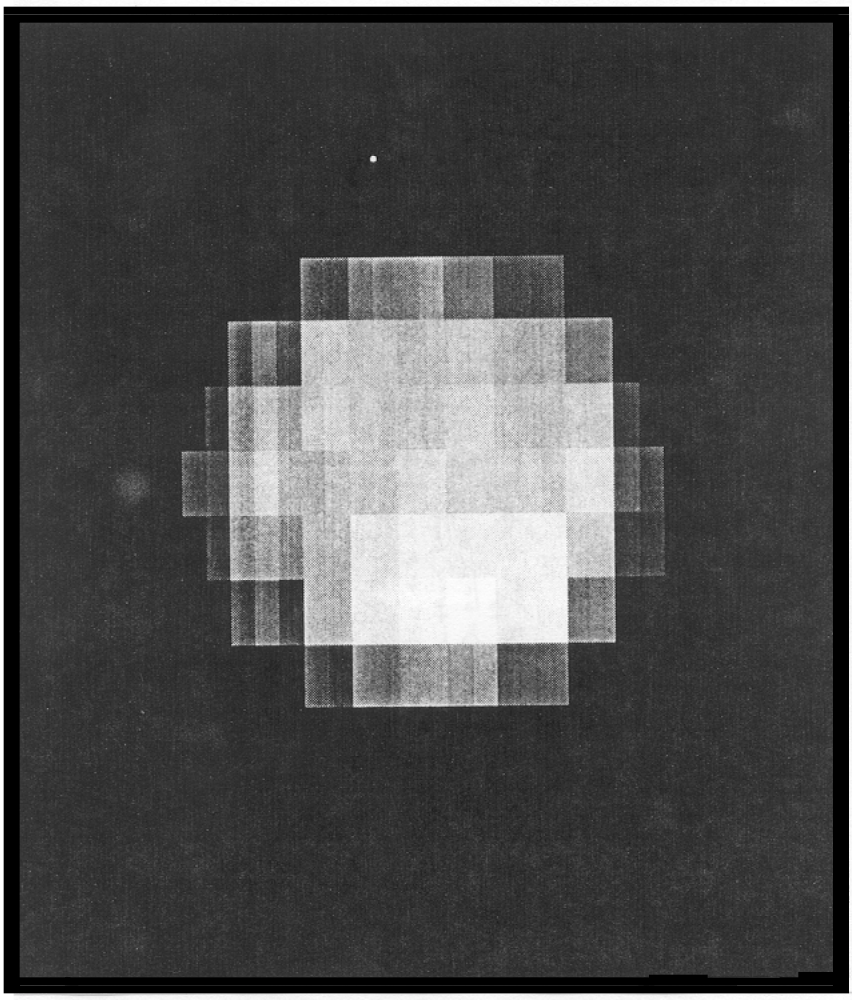

Fig. 22. Version 2 simulated lunar calibration data. The data were constructed from an actual scan of the moon by a ground-based SeaWiFS sensor in December, 1992.

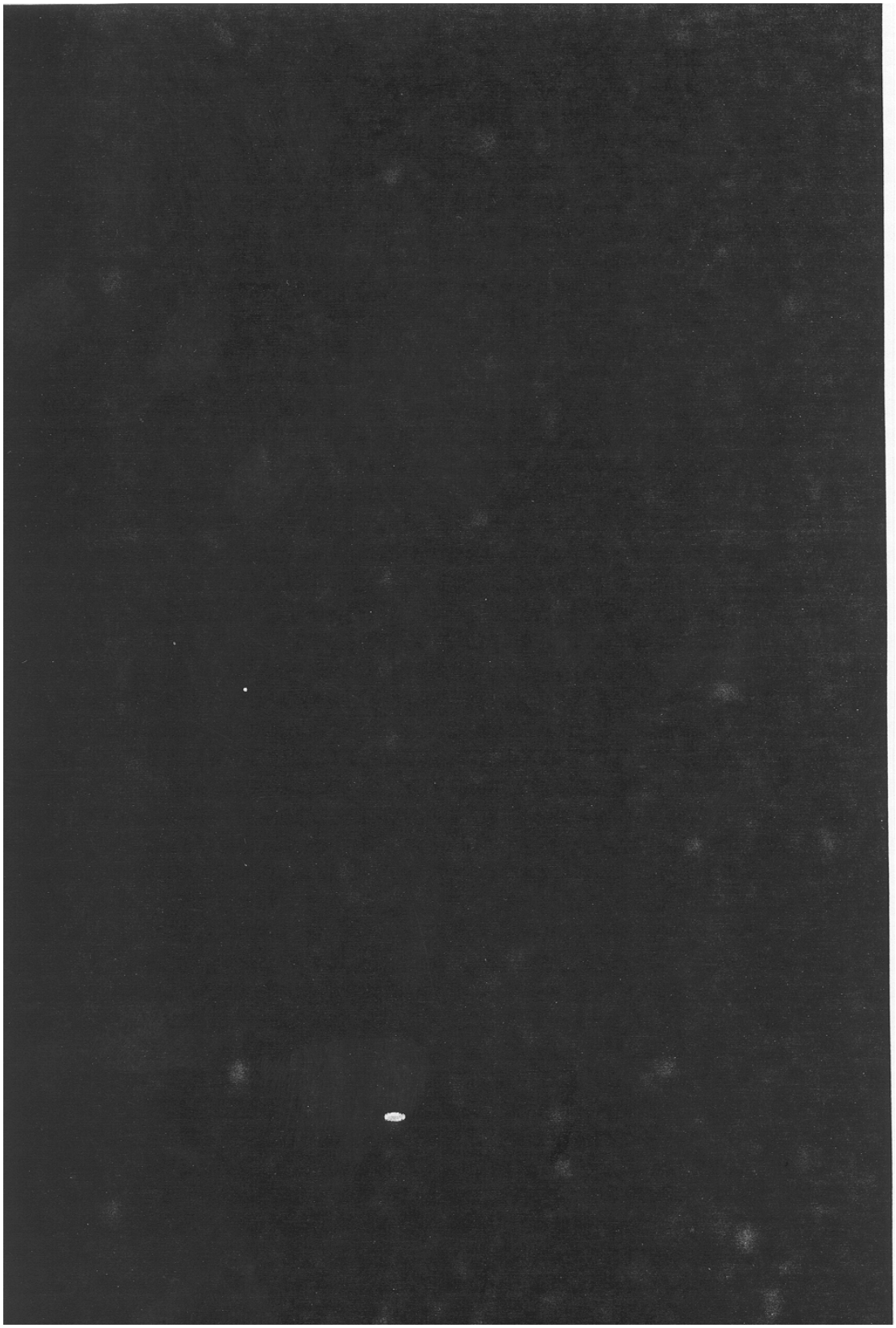

Fig. 23. This is how the lunar calibration data will appear in a recorded LAC segment.

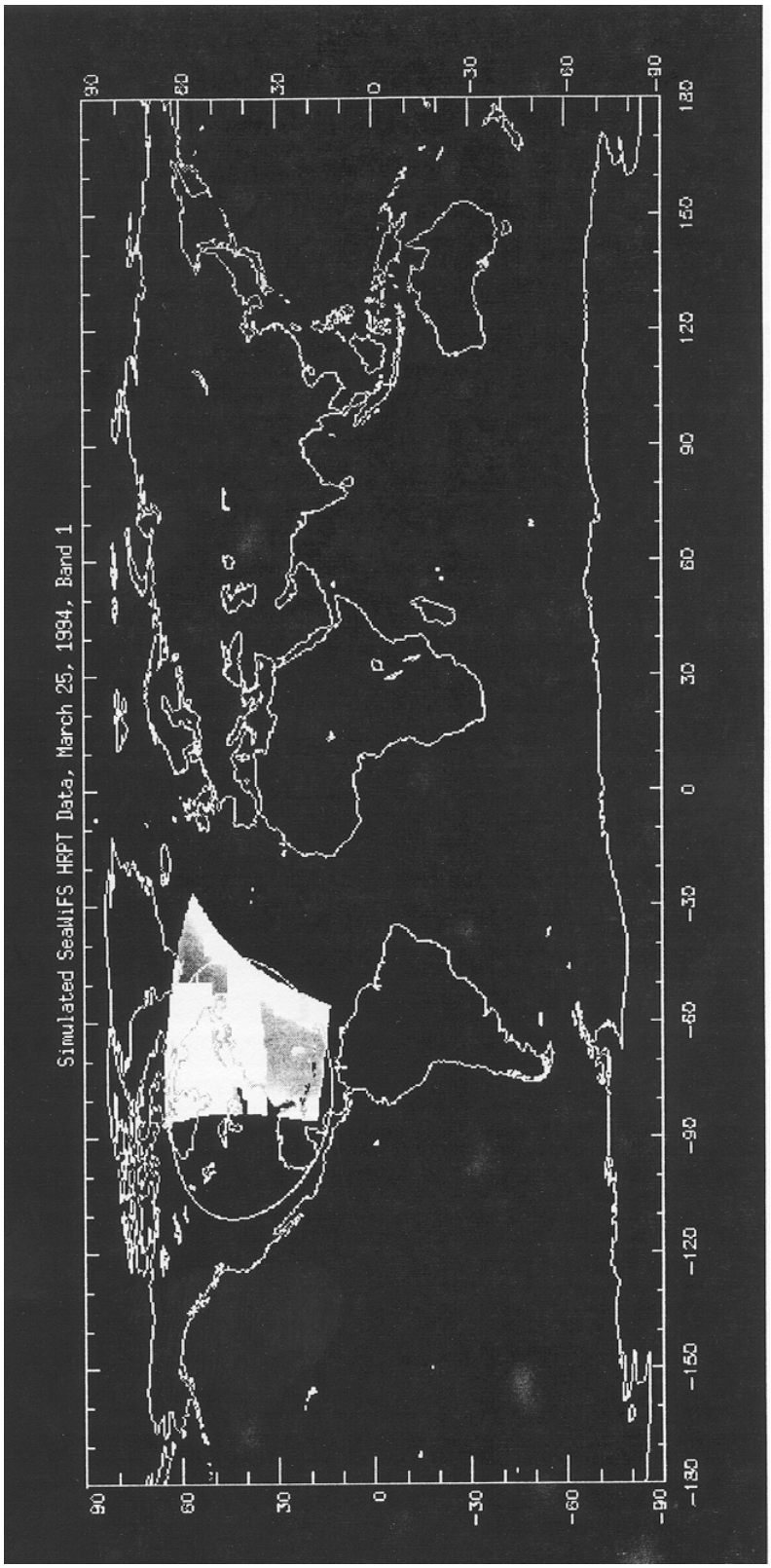

Fig. 24. Version 2 simulated SeaWiFS HRPT data over the GSFC station for March 25, 1994, band 1. This overpass corresponds to the GAC image shown earlier (Fig. 11). The GSFC visibility mask is also shown. The Earth-mapped data do not coincide with the visibility mask boundaries because the sensor is tilted.

Fig. 25. Version 2 segment of HRPT pass in satellite coordinates for band 1. This image corresponds to the GAC image in Fig. 13. Note the greater width of the LAC data, and the higher spatial resolution. The large white objects are clouds, but small white features on the islands are probably saturating beaches.

Fig. 26. As in Fig. 25 for band 8, where all land and clouds saturate. The high spatial resolution of the land and sea mask is apparent.

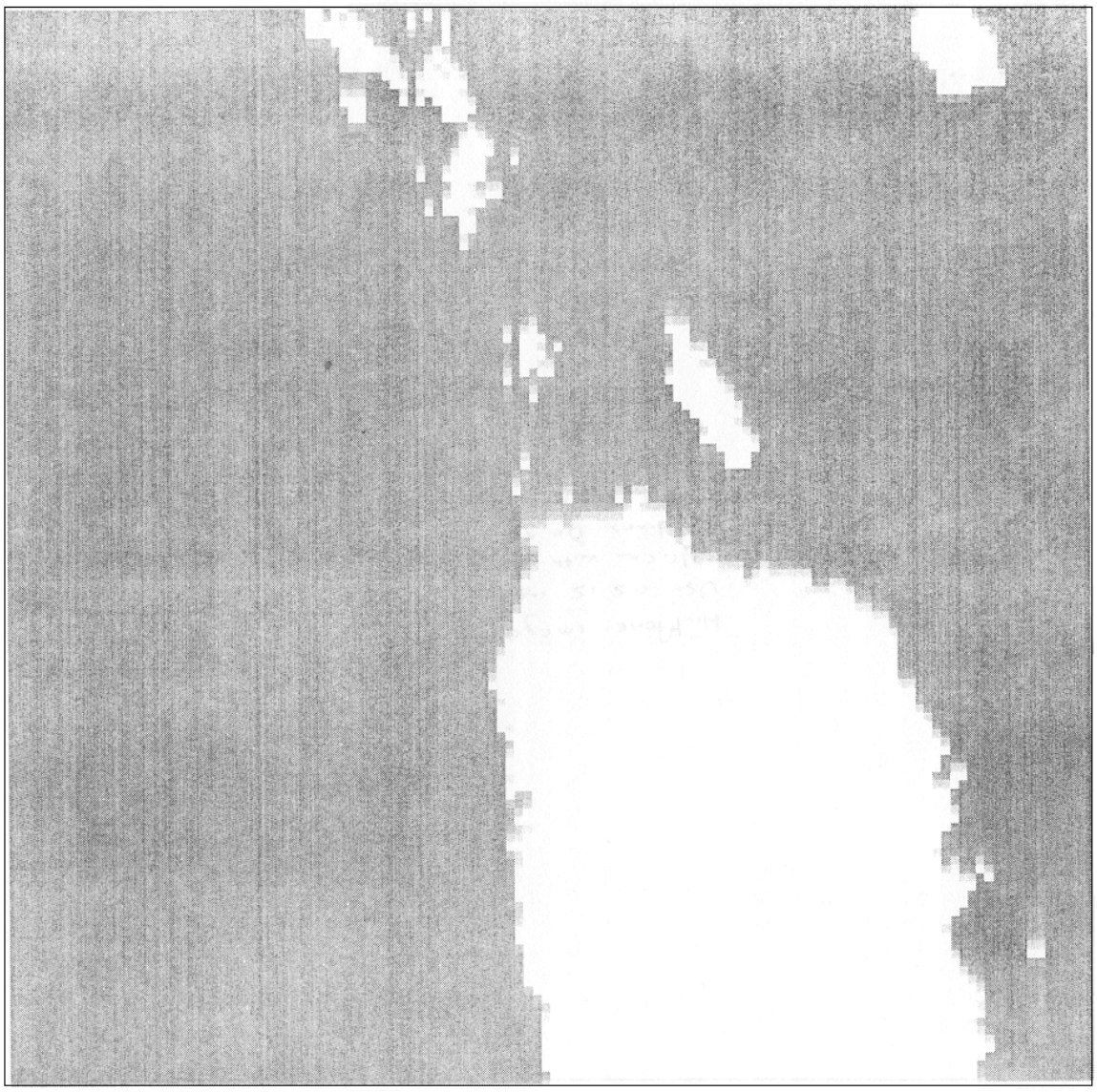

Fig. 27. Portion of a Version 2 HRPT pass over eastern Puerto Rico in band 8, showing sensor saturation features. *Ghost* pixels in diminishing magnitudes in both directions along scan away from islands leads to a blurring effect.

5. DATA AVAILABILITY

The data set containing 16-bit science data (frame formatter output or level-0 data) is available on Internet from the GSFC DAAC. The address is: eosdata.gsfc.nasa.gov. Log in as `anonymous` with password `guest`, then change directories to `pub/seawifs`. All files begin with `S` followed by the year, so all files belonging to this simulated data set (Version 2) will begin with `S1994`. GAC files end with the suffix `L0_GAC`, recorded LAC files with `L0_LAC` and HRPT files with `L0_HRPT`. Assistance may be obtained by dialing 301–286–3209. Please note that for the mission, authorization must be obtained before acquiring the data.

The data files containing 10-bit science data (onboard structure) were intended to be used internally for end-to-end system testing. The data are available from the authors on 4 mm tape for Silicon Graphics IRIX or Sun SunOS systems.

Acknowledgments

The authors are indebted to a large number of people for their assistance and advice which was required due to the complexity of this undertaking. They are in alphabetical order: Robert Barnes (Man Tech Environmental), Frank Corprew (Hughes-STX), Gene Feldman (GSFC), Mary James (GSFC), Ken Lambert (University of Maryland), Robert Mack (Hughes-STX), and George Riggs (Research and Data Systems, Corp.). We would also like to thank Wayne Esaias for critical comments on the manuscript, and for encouraging us to submit it despite the sensor modifications agreed upon after the completion of this effort. smallbreak

Glossary

AMC	Angular Momentum Compensation
AVHRR	Advanced Very High Resolution Radiometer
BTR	Bright Target Recovery
CZCS	Coastal Zone Color Scanner
DAAC	Distributed Active Archive Center
DCF	Data Capture Facility
ECEF	Earth-Centered Earth-Fixed
FNOC	Fleet Numerical Oceanography Center
FPA	Focal Point Assembly
GAC	Global Area Coverage
GMT	Greenwich Mean Time
GPS	Global Positioning System
GSFC	Goddard Space Flight Center
HRPT	High Resolution Picture Transmission
ICD	Interface Control Document
ISCCP	International Satellite Cloud Climatology Project
LAC	Local Area Coverage
LSB	Least Significant Bits
MSB	Most Significant Bits
NASA	National Aeronautics and Space Administration
NASCOM	NASA Communications
NCDS	NASA Climate Data System
NDVI	Normalized Difference Vegetation Index
NER	Noise Equivalent Radiance
NGDC	National Geophysical Data Center
NIMBUS	Not an acronym, a series of NASA experimental weather satellites containing a wide variety of atmosphere, ice, and ocean sensors.
NORAD	North American Air Defense (Command)
OSC	Orbital Sciences Corporation
PFF	Programmable Frame Formatter
QC	Quality Control
SBRC	(Hughes) Santa Barbara Research Center
S/C	Spacecraft
SDPS	SeaWiFS Data Processing System
SeaWiFS	Sea-viewing Wide Field-of-view Sensor
SOC	Simulation Operations Center
SOH	State of Health
TDI	Time-Delay and Integration
TOMS	Total Ozone Mapping Spectrometer
WFF	Wallops Flight Facility
WVS	World Vector Shoreline

Symbols

a	A constant equal to $-20/\tanh(2)$.
a_{o}	Oxygen absorption coefficient.
a_{oz}	Ozone absorption coefficient.
a_{wv}	Coefficient for water vapor absorption.
b	A constant equal to 1/3.
DC	Digital count value.
E_d	Incident downwelling irradiance.
$F_0(\lambda)$	Mean extraterrestrial spectral irradiance.
G	Gain factor.
$L_{\mathrm{NER}}\lambda)$	Noise equivalent radiance.
$L_{\mathrm{sat}}(\lambda)$	Saturation radiance for the sensor.
$L_t(\lambda)$	At-satellite radiance.
M	Atmospheric slant path length.
P	Local surface pressure.
P_0	Standard pressure.
$s(\lambda)$	Slope for the range 0–1,023.
t	Time in seconds.
T	Tilt position.
V	Volts.
X	ECEF X component of orbit position.
$\dot{X}$	ECEF X component of orbit velocity.
Y	ECEF Y component of orbit position.
$\dot{Y}$	ECEF Y component of orbit velocity.
Z	ECEF Z component of orbit position.
$\dot{Z}$	ECEF Z component of orbit velocity.
λ	Wavelength of light.
Ψ	Yaw.
$\dot{\Psi}$	Yaw rate.
Φ	Roll.
$\dot{\Phi}$	Roll rate.
$\rho_{c,i}$	Reflectance of clouds and ice.
θ	Pitch.
$\dot{\theta}$	Pitch rate.
θ_0	Solar zenith angle.
τ_r	Rayleigh optical thickness.
τ_r'	Pressure corrected Rayleigh optical thickness.
τ_{ro}	Rayleigh optical thickness weighted by the SeaWiFS spectral response.

References

Gordon, H.R., J.W. Brown, and R.H. Evans, 1988: Exact Rayleigh scattering calculations for use with the Nimbus-7 Coastal Zone Color Scanner. *Appl. Opt.,* 862–871.

Gregg, W.W., and K.L. Carder, 1990: A simple spectral solar irradiance model for cloudless maritime atmospheres. *Limnol. Ocean.,* 1,657–1,675.

——, F. Chen, A. Mezaache, J. Chen, and J. Whiting, 1993: The simulated SeaWiFS data set: Version 1. *NASA Tech. Memo. 104566, Vol. 9,* S.B. Hooker and E.R. Firestone, Eds., NASA Goddard Space Flight Center, Greenbelt, Maryland, 17 pp.

——, and F.S. Patt, 1993: Assessment of tilt capability for spaceborne global ocean color sensors. *IEEE Trans. Geosci. Remote Sens.,* (submitted).

Patt, F.S., and W.W. Gregg, 1993: Exact closed-form geolocation algorithm for Earth survey sensors. *Inter. J. Remote Sens.,* (submitted).

Tucker, C.J., and L.D. Miller, 1977: Soil spectra contributions to grass canopy spectral reflectance. *Photogrammetry, Engineering, and Remote Sens.,* 721–726.

Wertz, J.R. (Ed.), 1978: *Spacecraft Attitude Determination and Control.* D. Reidel, Dordrecht, Holland, 858 pp.

Williams, S.P., E.F. Szajna, and W.A. Hovis, 1985: Nimbus 7 Coastal Zone Color Scanner (CZCS) level-1 data product users' guide. *NASA Tech. Memo. 86203,* NASA Goddard Space Flight Center, Greenbelt, Maryland, 49 pp.

Woodward, R.H., R.A. Barnes, C.R. McClain, W.E. Esaias, W.L. Barnes, and A.T. Mecherikunnel, 1993: Modeling of the SeaWiFS solar and lunar observations. *NASA Tech. Memo. 104566, Vol. 10,* S.B. Hooker and E.R. Firestone, Eds., 26 pp.

The SeaWiFS Technical Report Series

Vol. 1

Hooker, S.B., W.E. Esaias, G.C. Feldman, W.W. Gregg, and C.R. McClain, 1992: An Overview of SeaWiFS and Ocean Color. *NASA Tech. Memo. 104566, Vol. 1,* S.B. Hooker and E.R. Firestone, Eds., NASA Goddard Space Flight Center, Greenbelt, Maryland, 24 pp., plus color plates.

Vol. 2

Gregg, W.W., 1992: Analysis of Orbit Selection for SeaWiFS: Ascending vs. Descending Node. *NASA Tech. Memo. 104566, Vol. 2,* S.B. Hooker and E.R. Firestone, Eds., NASA Goddard Space Flight Center, Greenbelt, Maryland, 16 pp.

Vol. 3

McClain, C.R., W.E. Esaias, W. Barnes, B. Guenther, D. Endres, S. Hooker, G. Mitchell, and R. Barnes, 1992: Calibration and Validation Plan for SeaWiFS. *NASA Tech. Memo. 104566, Vol. 3,* S.B. Hooker and E.R. Firestone, Eds., NASA Goddard Space Flight Center, Greenbelt, Maryland, 41 pp.

Vol. 4

McClain, C.R., E. Yeh, and G. Fu, 1992: An Analysis of GAC Sampling Algorithms: A Case Study. *NASA Tech. Memo. 104566, Vol. 4,* S.B. Hooker and E.R. Firestone, Eds., NASA Goddard Space Flight Center, Greenbelt, Maryland, 22 pp., plus color plates.

Vol. 5

Mueller, J.L., and R.W. Austin, 1992: Ocean Optics Protocols. *NASA Tech. Memo. 104566, Vol. 5,* S.B. Hooker and E.R. Firestone, Eds., NASA Goddard Space Flight Center, Greenbelt, Maryland, 43 pp.

Vol. 6

Firestone, E.R., and S.B. Hooker, 1992: SeaWiFS Technical Report Series Summary Index: Volumes 1–5. *NASA Tech. Memo. 104566, Vol. 6,* S.B. Hooker and E.R. Firestone, Eds., NASA Goddard Space Flight Center, Greenbelt, Maryland, 9 pp.

Vol. 7

Darzi, M., 1992: Cloud Screening for Polar Orbiting Visible and IR Satellite Sensors. *NASA Tech. Memo. 104566, Vol. 7,* S.B. Hooker and E.R. Firestone, Eds., NASA Goddard Space Flight Center, Greenbelt, Maryland, 7 pp.

Vol. 8

Hooker, S.B., W.E. Esaias, and L.A. Rexrode, 1993: Proceedings of the First SeaWiFS Science Team Meeting. *NASA Tech. Memo. 104566, Vol. 8,* S.B. Hooker and E.R. Firestone, Eds., NASA Goddard Space Flight Center, Greenbelt, Maryland, 61 pp.

Vol. 9

Gregg, W.W., F.C. Chen, A.L. Mezaache, J.D. Chen, J.A. Whiting, 1993: The Simulated SeaWiFS Data Set, Version 1. *NASA Tech. Memo. 104566, Vol. 9,* S.B. Hooker and E.R. Firestone, Eds., NASA Goddard Space Flight Center, Greenbelt, Maryland, 17 pp.

Vol. 10

Woodward, R.H., R.A. Barnes, C.R. McClain, W.E. Esaias, W.L. Barnes, and A.T. Mecherikunnel, 1993: Modeling of the SeaWiFS Solar and Lunar Observations. *NASA Tech. Memo. 104566, Vol. 10,* S.B. Hooker and E.R. Firestone, Eds., NASA Goddard Space Flight Center, Greenbelt, Maryland, 26 pp.

Vol. 11

Patt, F.S., C.M. Hoisington, W.W. Gregg, and P.L. Coronado, 1993: Analysis of Selected Orbit Propagation Models for the SeaWiFS Mission. *NASA Tech. Memo. 104566, Vol. 11,* S.B. Hooker, E.R. Firestone, and A.W. Indest, Eds., NASA Goddard Space Flight Center, Greenbelt, Maryland, 16 pp.

Vol. 12

Firestone, E.R., and S.B. Hooker, 1993: SeaWiFS Technical Report Series Summary Index: Volumes 1–11. *NASA Tech. Memo. 104566, Vol. 12,* S.B. Hooker and E.R. Firestone, Eds., NASA Goddard Space Flight Center, Greenbelt, Maryland, 28 pp.

Vol. 13

McClain, C.R., K.R. Arrigo, J. Comiso, R. Fraser, M. Darzi, J.K. Firestone, B. Schieber, E-n. Yeh, and C.W. Sullivan, 1993: Case Studies for SeaWiFS Calibration and Validation, Part 1. *NASA Tech. Memo. 104566, Vol. 13,* S.B. Hooker and E.R. Firestone, Eds., NASA Goddard Space Flight Center, Greenbelt, Maryland, 52 pp., plus color plates.

Vol. 14

Mueller, J.L., 1993: The First SeaWiFS Intercalibration Round-Robin Experiment, SIRREX-1, July 1992. *NASA Tech. Memo. 104566, Vol. 14,* S.B. Hooker and E.R. Firestone, Eds., NASA Goddard Space Flight Center, Greenbelt, Maryland, 60 pp.

Vol. 15

Gregg, W.W., F.S. Patt, R.H. Woodward, 1993: The Simulated SeaWiFS Data Set, Version 2. *NASA Tech. Memo. 104566, Vol. 15,* S.B. Hooker and E.R. Firestone, Eds., NASA Goddard Space Flight Center, Greenbelt, Maryland, 42 pp., plus color plates.

COLOR PLATES

The following color plates are presented *as submitted* by the authors.

Plate 1. Top: Simulated SeaWiFS GAC data, 25 March 1994, band 1, mapped to Earth coordinates. Bottom: band 8.

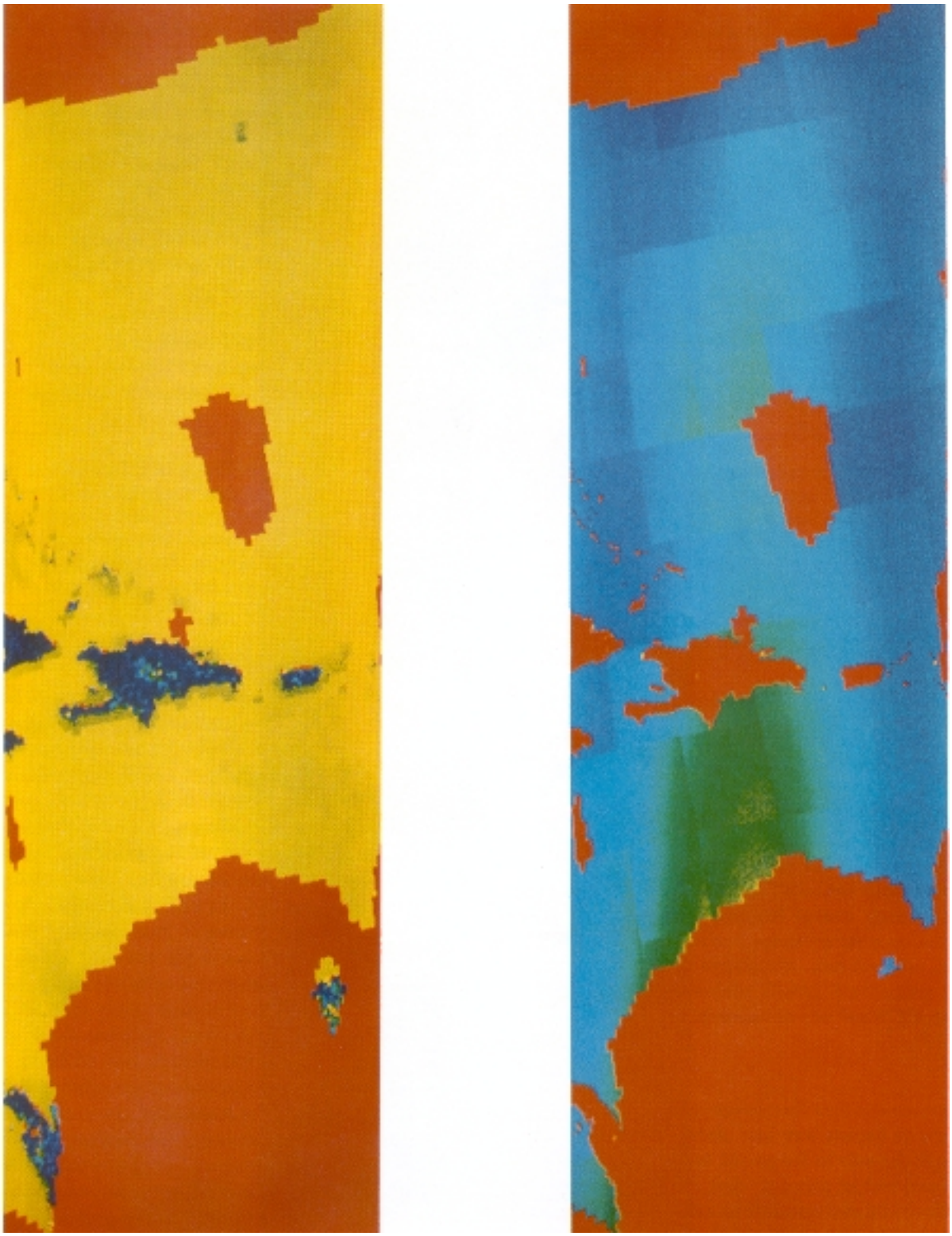

PLATE 2. Left: A portion of simulated SeaWiFS GAC data, band 1, in satellite coordinates (i.e., scan is x axis, orbit propagation direction is y axis). The Dominican Republic and Haiti is the dark blue object near the center of the image, with Puerto Rico to the east. The color scale indicates low at-satellite radiance (dark blue) to high radiance (bright red). All of the bright red objects in this image are clouds. Left: band 8. Land features are saturated in band 8.

PLATE 3. Recorded LAC segments shown in Fig. 16, of band 1, in satellite coordinates. The first segment is over Saudi Arabia, and the second over South Africa.

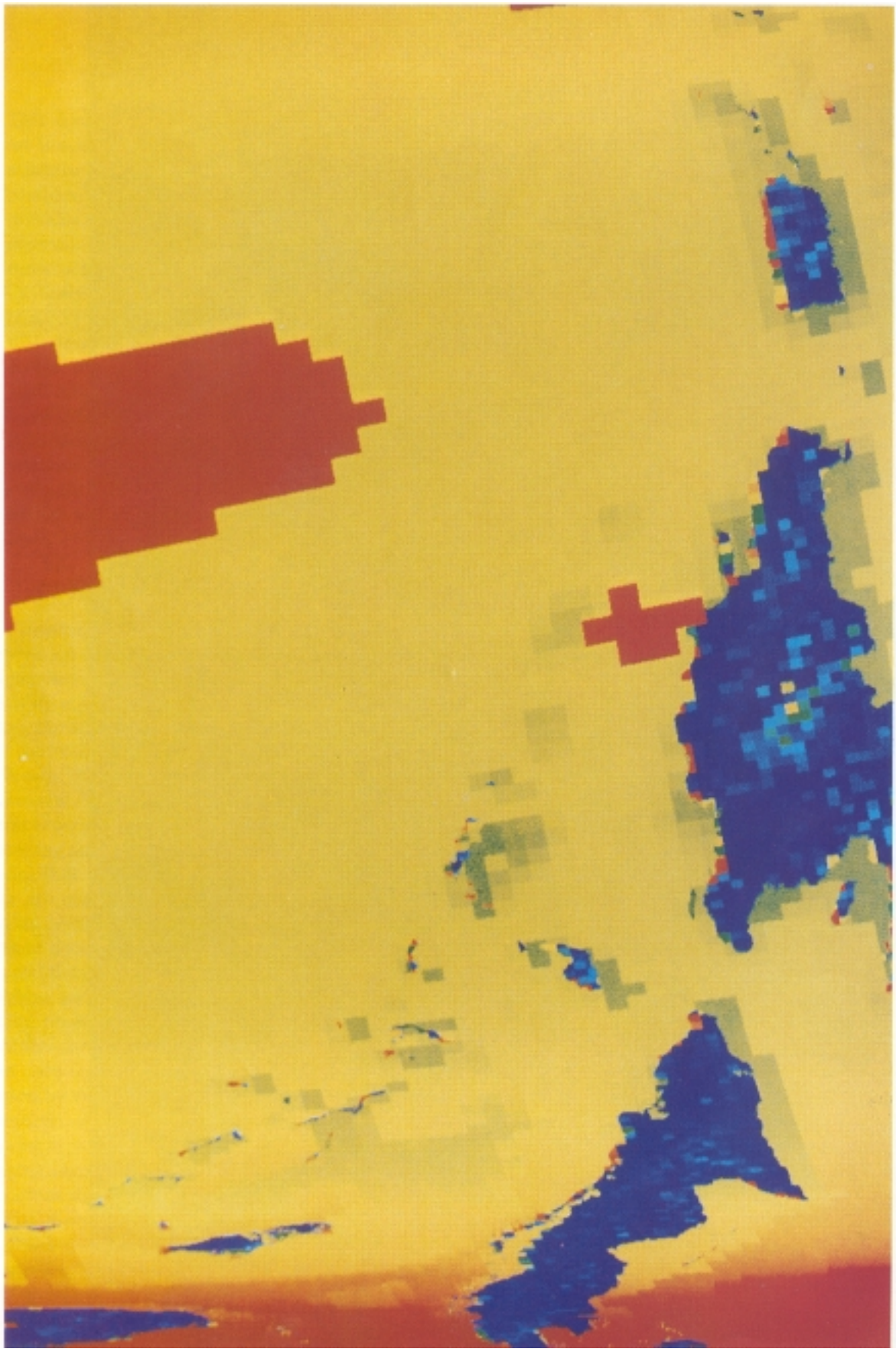

PLATE 4. Segment of HRPT pass in satellite coordinates for band 1. This image corresponds to the GAC image in Fig. 13. Note the greater width of the LAC data, and the higher spatial resolution. The large red objects are clouds, but small red features on the islands are probably saturating beaches.

PLATE 5. As in Plate 4 for band 8, where all land and clouds saturate. The high spatial resolution of the land and sea mask is apparent.

PLATE 6. Portion of HRPT pass over eastern Puerto Rico in band 8, showing sensor saturation features. *Ghost* pixels, in diminishing magnitudes in both directions along scan away from islands, leads to a blurring effect.

REPORT DOCUMENTATION PAGE

Form Approved
OMB No. 0704-0188

1. AGENCY USE ONLY *(Leave blank)*	2. REPORT DATE	3. REPORT TYPE AND DATES COVERED
	January 1994	Technical Memorandum

4. TITLE AND SUBTITLE
SeaWiFS Technical Report Series
Volume 15–The Simulated SeaWiFS Data Set, Version 2

5. FUNDING NUMBERS

6. AUTHOR(S)
Watson W. Gregg, Frederick S. Patt, and Robert H. Woodward

Series Editors: Stanford B. Hooker and Elaine R. Firestone

7. PERFORMING ORGANIZATION NAME(S) AND ADDRESS(ES)
Laboratory for Hydrospheric Processes
Goddard Space Flight Center
Greenbelt, Maryland 20771

8. PERFORMING ORGANIZATION REPORT NUMBER
94B00041
Code 970.2

9. SPONSORING/MONITORING AGENCY NAME(S) AND ADDRESS(ES)
National Aeronautics and Space Administration
Washington, D.C. 20546–0001

10. SPONSORING/MONITORING AGENCY REPORT NUMBER
TM–104566, Vol. 15

11. SUPPLEMENTARY NOTES
Frederick S. Patt, Robert H. Woodward, and Elaine R. Firestone: General Sciences Corporation, Laurel, Maryland.

12a. DISTRIBUTION/AVAILABILITY STATEMENT
Unclassified–Unlimited
Subject Category 48
Report is available from the Center for AeroSpace Information (CASI),
7121 Standard Drive, Hanover, MD 21076–1320; (301)621-0390

12b. DISTRIBUTION CODE

13. ABSTRACT *(Maximum 200 words)*

This document describes the second version of the simulated SeaWiFS data set. A realistic simulated data set is essential for mission readiness preparations and can potentially assist in all phases of ground support for a future mission. The second version improves on the first version primarily through additional realism and complexity. This version incorporates a representation of virtually every aspect of the flight mission. Thus, it provides a high-fidelity data set for testing several aspects of the ground system, including data acquisition, data processing, data transfers, calibration and validation, quality control, and mission operations. The data set is constructed for a seven-day period, 25–31 March 1994. Specific features of the data set include Global Area Coverage (GAC), recorded Local Area Coverage (LAC), and real-time High Resolution Picture Transmission (HRPT) data for the seven-day period. A realistic orbit, which is propagated using a Brouwer-Lyddane model with drag, is used to simulate orbit positions. The simulated data corresponds to the command schedule based on the orbit for this seven-day period. It includes total (at-satellite) radiances not only for ocean, but for land, clouds, and ice. The simulation also utilizes a high-resolution land-sea mask. It includes the April 1993 SeaWiFS spectral responses and sensor saturation responses. The simulation is formatted according to July 1993 onboard data structures, which include corresponding telemetry (instrument and spacecraft) data. The methods are described and some examples of the output are given. The instrument response functions made available in April 1993 have been used to produce the Version 2 simulated data. These response functions will change as part of the sensor improvements initiated in July–August 1993.

14. SUBJECT TERMS
SeaWiFS, Oceanography, GAC Data, LAC Data, Orbit Propagation, Navigation, Command Schedules, At-Satellite Radiances, Sensor Saturation Response, Data Formatting, HRPT Data

15. NUMBER OF PAGES
51

16. PRICE CODE

17. SECURITY CLASSIFICATION OF REPORT	18. SECURITY CLASSIFICATION OF THIS PAGE	19. SECURITY CLASSIFICATION OF ABSTRACT	20. LIMITATION OF ABSTRACT
Unclassified	Unclassified	Unclassified	Unlimited